

Precision calculation of critical exponents in the $O(N)$ universality classes with the nonperturbative renormalization group

Gonzalo De Polsi,¹ Ivan Balog,² Matthieu Tissier,³ and Nicolás Wschebor⁴

¹*Instituto de Física, Facultad de Ciencias, Universidad de la República, Iguá 4225, 11400, Montevideo, Uruguay*

²*Institute of Physics, Bijenička cesta 46, HR-10001 Zagreb, Croatia*

³*Sorbonne Université, CNRS, Laboratoire de Physique Théorique de la Matière Condensée, LPTMC, F-75005 Paris, France*

⁴*Instituto de Física, Facultad de Ingeniería, Universidad de la República, J.H.y Reissig 565, 11000 Montevideo, Uruguay*

(Dated: January 22, 2020)

We compute the critical exponents ν , η and ω of $O(N)$ models for various values of N by implementing the derivative expansion of the nonperturbative renormalization group up to next-to-next-to-leading order [usually denoted $\mathcal{O}(\partial^4)$]. We analyze the behavior of this approximation scheme at successive orders and observe an apparent convergence with a small parameter – typically between $1/9$ and $1/4$ – compatible with previous studies in the Ising case. This allows us to give well-grounded error bars. We obtain a determination of critical exponents with a precision which is similar or better than those obtained by most field theoretical techniques. We also reach a better precision than Monte-Carlo simulations in some physically relevant situations. In the $O(2)$ case, where there is a longstanding controversy between Monte-Carlo estimates and experiments for the specific heat exponent α , our results are compatible with those of Monte-Carlo but clearly exclude experimental values.

I. INTRODUCTION

Systems where microscopic degrees of freedom are strongly coupled are notoriously difficult to analyze theoretically. This difficulty becomes even more involved if the system is near a critical point because of the large number of interacting degrees of freedom that must be treated simultaneously. From the theoretical viewpoint, two methods are widely used to study these physical situations. The first one was introduced by Wilson: the Renormalization Group (RG) [1]. This technique, when used in conjunction with perturbation theory is able to describe systems with many interacting degrees of freedom with a small or moderate effective coupling among infrared degrees of freedom. The perturbative implementation of the RG [2, 3] has become a fantastic method both in statistical physics and in quantum field theory when very different scales are present [4]. In the realm of statistical physics, it has been used to describe both equilibrium and out-of-equilibrium situations, it can deal with quenched disorder, long range interactions, etc. A main limitation of this approach is that it is based on an expansion in some small coupling and it cannot be applied to systems where no such small parameter is known. Moreover, the algebraic complexity of the calculation strongly increases with the order of the expansion. Due to this complexity, only recently progress have been done [5] and the perturbative series have been pushed to 7 loops. Another limitation of perturbative RG is that the series do not converge in general and one has to resort to some resummation techniques in order to make precise predictions. These techniques always involve some unknown parameters that must be fixed by using some extra criterion, such as the principle of minimal sensitivity or the principle of fastest apparent convergence, see below.

The other popular theoretical approach to critical systems is computer simulations [6]. A major asset of these techniques is their versatility: they can be applied to a large number of situations – at criticality or away from criticality – even when perturbative RG treatment might be very difficult. At a quantitative level, high precision estimates of the critical exponents were obtained by these methods, see [3] for a review. A major drawback is that it can require extremely large amounts of computer time and statistical and systematic errors only decrease slowly with the size of the simulation. To give an example, for the Monte-Carlo studies of criticality of the pure Ising model, which are considered to be the most favorable case numerically, the most extensive numerical study [7] reaches lattice sizes of $L = 300$ in 3d, for which 30 years of CPU time are needed. In the case of the most recent simulation on the XY model [8], on which we comment later on, the numerical load is approximately four times bigger.

There also exist methods which apply only to some particular physical situations. Among these, let us cite the large- N expansion, high- and low-temperature expansions. The other method of choice for studying critical exponents is conformal field theory [9, 10] which can be applied to a variety of systems at equilibrium in their critical regime, which present, on top of scale invariance the whole conformal group. These methods were first developed in the bidimensional case but were more recently applied to higher dimensions, through the Conformal Bootstrap (CB) program [11–13]. This led in the recent past to an unprecedented precision on critical exponents for the Ising model. Such methods are however unable to access other quantities of physical interest, such as a phase diagram.

The two versatile methods mentioned above – perturbative renormalization-group and lattice simulations – have both their limitations. In order to overcome some

of these, a third, flexible, method was developed in the 90's [14–18]. It is known as the nonperturbative RG (NPRG hereafter) or “functional RG” or, even “exact RG”. It is nowadays widely used in particle physics, solid state physics, statistical mechanics in and out of equilibrium, quantum gravity, etc. We shall describe the NPRG in more details below but, in a nutshell, it is based on an exact RG equation which describes the evolution of an effective average action when more and more short-distance fluctuations are integrated over. This equation is too complex to be solved exactly. In actual calculations, the strategy consists in looking for approximate solution to this exact equation: instead of considering the full functional dependence of the effective average action, one retains only a subset of coupling constants and looks for (approximate) solutions within this subset. The most popular approximation scheme is the Derivative Expansion (DE). It consists in classifying the terms appearing in the effective average action according to the number of gradients they contain and retaining only those with up to s gradients. We refer to this approximation as DE at order $\mathcal{O}(\partial^s)$ and the leading approximation, where all derivatives of the field are depreciated, except for a unrenormalized gradient $(\partial\phi)^2$ is called the Local Potential Approximation (LPA). This is equivalent to saying that the n -point vertex functions are expanded in powers of the momenta, up to order p^s . Such an expansion is justified if one is interested in the long-distance properties of the system, see below for more detail.

What is remarkable about the NPRG is that it is very resilient: even quite crude truncations can lead to qualitatively correct physics. Until recently, a major drawback of the method was that only limited knowledge was available concerning the convergence of the results when richer truncations were considered. This situation changed last year [19], when it was shown, in the case of the Ising model, that the results in the DE should converge with a convergence parameter in-between 1/4 and 1/9, which is indeed not too large. This theoretical prediction was checked explicitly by computing critical exponents η and ν in the derivative expansion pushed up to $\mathcal{O}(\partial^6)$. The output of this study is the determination of the critical exponents $\nu = 0.6300(2)$ and $\eta = 0.0358(6)$. Remarkably, these are in excellent agreement with CB values $\nu = 0.629971(4)$ and $\eta = 0.0362978(20)$ [13], and better than perturbative 6-loop ones [2]. This is an important breakthrough which shows that the NPRG can be used to obtain precise determinations of critical exponents, with well-grounded error bars. Note that critical exponents are just one example of physical quantities that can be computed by NPRG methods. They provide a good benchmarks to test the convergence of DE because other methods, such as CB and MC, yield very precise determinations of these quantities. NPRG, however, can be used to determine other physical quantities, such as a critical temperature, scaling functions and we expect that the convergence of the DE is governed by the same small parameter, of the order of 1/4 to 1/9.

Our aim in this paper is twofold. We first show that the convergence of the DE in $O(N)$ models is similar to what was found in the Ising case, with a convergence parameter in-between 1/4 and 1/9. This is checked explicitly by looking at the convergence of the DE expansion up to $\mathcal{O}(\partial^4)$ for the critical exponents η and ν . We also treat the correction to scaling exponent ω which was not considered in [19].¹ This enables us to determine convincing error bars. We describe in detail the methodology used to determine error bars because it is quite generic and could be used in many applications of the NPRG. The second aim of this article is to determine the critical exponents for different values of N . This is not only an academic issue because the $O(N)$ universality classes for $N=1, 2, 3$ and 4 have direct physical realizations [4]. Additionally the limits $N \rightarrow 0$ and $N \rightarrow -2$ are also of physical interest, being related to self avoiding random walks [20] and loop erased random walks [21, 22] respectively.

The $N = 2$ case is of particular interest because it describes the normal to superfluid transition in Helium-4. Experimental methods led to a determination of the critical exponent which governs the singularity of the specific heat with unprecedented precision. By using hyperscaling relation, this yields an exponent $\nu = 0.6709(1)$ [23]. The main limitation on experiments was the variation of the density of the fluid within the sample caused by gravity and it was necessary to perform the experiment in the Space Shuttle in order to obtain a sufficiently homogeneous system.

This high precision experiment triggered an important theoretical effort to obtain a determination of critical exponents with a similar precision. What is curious is that there exists a discrepancy between the experimental and the most precise Monte-Carlo results [8], which reports $\nu = 0.67169(7)$. These two results are not compatible. Other field-theoretical results based on perturbative renormalization-group led to too large error bars to settle the controversy. One of the main results of this article is the determination of the critical exponent $\nu = 0.6716(6)$ which is compatible with Monte-Carlo results, but not with experimental ones. We should mention that, during the completion of this article, a theoretical result based on CB was reported [24], which leads to the same conclusion, see below for more detail.

The article is organized as follows. We present the NPRG method and the approximation scheme (the DE) that we implement in Sect. II. We then review the analysis of the Ising case in Sect. III presented in Ref. [19]. Sect. IV is devoted to the description of the methodology proposed to estimate error bars. In Sect. V, we give our determinations of the critical exponents for various values of N , including the physical cases $N = 2, 3$ as well as the non-unitary cases $N = 0$ and $N = -2$. We also test

¹ The authors of [19] had studied this exponent for $N = 1$ but did not publish it. We acknowledge discussion with them on this topic.

large values of N to compare with the large- N results. Some technical details are addressed in Appendices.

II. NON-PERTURBATIVE RENORMALIZATION GROUP AND DERIVATIVE EXPANSION

A. The Non-Perturbative Renormalization Group

We start with a brief review of the NPRG. It is based on Wilson's ideas of integrating first the highly oscillating modes (i.e. those with a wave-vector larger than some scale k) while the long-distance modes are frozen.

A convenient implementation of this consists in adding to the Euclidean action (or Hamiltonian) a regulating term, quadratic in the fields and dependent on a momentum scale k [25], $S[\varphi] \rightarrow S[\varphi] + \Delta S_k[\varphi]$ with:

$$\Delta S_k[\varphi] = \frac{1}{2} \int_{x,y} \varphi_a(x) R_k(x,y) \varphi_a(y), \quad (1)$$

where $\int_x = \int d^d x$. The regulating function R_k is chosen to be invariant under rotations and translations and therefore depends only on $|x - y|$. Here and below, Einstein convention is adopted both on sums over internal and space indices. To properly regularize the theory in the infrared, the Fourier transform $R_k(q)$ of $R_k(x - y)$ should:

- be a smooth function of the modulus of the momentum q ;
- behave as a "mass square" of order k^2 for long-distance modes: $R_k(q) \sim Z_k k^2$ for $q \ll k$, where Z_k is a field renormalization factor to be specified below;
- go to zero rapidly when $q \gg k$ (typically faster than any power law).

With these properties the term (1) regularizes the theory in the infrared without modifying the ultraviolet regime. One can then define a scale-dependent partition function in the presence of an arbitrary external source J [14–16]:

$$\mathcal{Z}_k[J] = e^{W_k[J]} = \int \mathcal{D}\varphi e^{-S[\varphi] - \Delta S_k[\varphi] + \int_x J_a(x) \varphi_a(x)}, \quad (2)$$

where $W_k[J]$ is the Helmholtz free-energy or generating functional of connected correlation functions. The Gibbs free-energy, or scale-dependent effective action, is defined as the modified Legendre transform of $W_k[J]$:

$$\Gamma_k[\phi] = \int_x \phi_a(x) J_a(x) - W_k[J] - \Delta S_k[\phi]. \quad (3)$$

In the previous equation, J is an implicit function of ϕ , obtained by inverting

$$\phi_a(x) = \frac{\delta W_k}{\delta J_a(x)}. \quad (4)$$

The theory is defined at a microscopic scale Λ as the inverse of lattice spacing. $\Gamma_k[\phi]$ is the generating functional of IR-regularized proper vertices defined as

$$\Gamma_{a_1 \dots a_n}^{(n)}[x_1, \dots, x_n; \phi] = \frac{\delta^n \Gamma_k[\phi]}{\delta \phi_{a_1}(x_1) \dots \delta \phi_{a_n}(x_n)}. \quad (5)$$

Here and below, we have omitted to indicate the k -dependence of the regularized proper vertices to alleviate notation. As is well-known only 1PI perturbative diagrams contribute to proper vertices. In actual calculations, we will be interested in proper vertices evaluated in a uniform field. We therefore define

$$\Gamma_{a_1 \dots a_n}^{(n)}(x_1, \dots, x_n; \phi) = \Gamma_{a_1 \dots a_n}^{(n)}[x_1, \dots, x_n; \phi(x)] \Big|_{\phi(x) \equiv \phi}. \quad (6)$$

The Fourier transform of the vertices are defined as:

$$\begin{aligned} \Gamma_{a_1 \dots a_n}^{(n)}(p_1, \dots, p_{n-1}; \phi) \\ = \int_{x_1 \dots x_{n-1}} e^{i \sum_{m=1}^{n-1} x_m \cdot p_m} \Gamma_{a_1 \dots a_n}^{(n)}(x_1, \dots, x_{n-1}, 0; \phi). \end{aligned} \quad (7)$$

which only depend on $n - 1$ independent wave-vectors because of the invariance under translations.

The evolution of $\Gamma_k[\phi]$ with the RG time $t = \log(k/\Lambda)$ [14–16] can be easily obtained:

$$\partial_t \Gamma_k[\phi] = \frac{1}{2} \int_{x,y} \partial_t R_k(x-y) G_{aa}[x,y;\phi] \quad (8)$$

where $G_{ab}[x,y;\phi]$ is the propagator in an arbitrary external field $\phi(x)$, which has a matrix structure because of the internal indices. Here again, we omit to indicate the k -dependence of the propagator to alleviate notations. The propagator can be obtained from the two-point vertex in a standard way:

$$\int_y G_{ac}[x,y;\phi] \left[\Gamma_{cb}^{(2)}[y,z;\phi] + R_k(y-z) \delta_{cb} \right] = \delta(x-z) \delta_{ab} \quad (9)$$

The exact flow equation (8) is a nonlinear functional equation. From this functional equation, one can derive equations for the various proper vertices. For instance, evaluating (8) in a uniform external field one deduces the exact equation for the effective potential (or 0-point vertex in a uniform field ϕ):

$$\partial_t U_k(\phi) = \frac{1}{2} \int_q \partial_t R_k(q) G_{aa}(q; \phi). \quad (10)$$

As for the potential, the equation for the 2-point function in a uniform external field can be deduced by taking two functional derivatives of (8) and then evaluating in a uniform field. This gives, after Fourier transform:

$$\begin{aligned} \partial_t \Gamma_{ab}^{(2)}(p; \phi) = \int_q \partial_t R_k(q) G_{mn}(q; \phi) \left\{ -\frac{1}{2} \Gamma_{abns}^{(4)}(p, -p, q; \phi) \right. \\ \left. + \Gamma_{anl}^{(3)}(p, q; \phi) G_{lr}(p+q; \phi) \Gamma_{bsr}^{(3)}(-p, -q; \phi) \right\} G_{sm}(q\phi) \end{aligned} \quad (11)$$

Similarly, one can deduce the equation for any vertex function. As is well-known, it leads to an infinite hierarchy of coupled equations, where the equation for $\Gamma^{(n)}$ depends on all the vertices up to $\Gamma^{(n+2)}$. As a consequence Eq. (8), or equivalently, the infinite hierarchy for vertex functions cannot be solved without approximations, in the most interesting cases.

The asset of Eq. (8) compared to other functional equations is that it is well-suited to formulate approximations going beyond perturbation theory. In particular,

- It has a one-loop structure written exclusively in terms of running and regularized vertices extracted from Γ_k .
- It has a 1PI structure (only dressed 1PI diagrams contribute).
- In Fourier space, only internal momenta $q \lesssim k$ contribute significantly to the flows of any vertex.

This structure is clearly visible in the equations (10) and (11) for the effective potential and 2-point vertex and one can easily see that the same property holds for any vertex-function.

In the next paragraph we present the most studied approximation going beyond perturbation theory within the NPRG: the DE. It fully exploits the specific properties of the NPRG that we just mentioned.

B. The Derivative Expansion

The DE procedure consists in taking an *ansatz* for the effective action $\Gamma_k[\phi]$ in which only terms with a finite number of derivatives of the fields appear. Equivalently, in Fourier space, it corresponds to expanding all proper vertices in power series of the momenta and truncating to a finite order. This approximation is only well-suited for studying the long-distance properties of the system since higher momentum dependence are neglected. In fact, it proved to be a good approximation scheme for \mathbb{Z}_2 and $O(N)$ models with a very good level of precision (see for example, [17, 19, 26, 27]). One of the reasons for the success of the DE in $O(N)$ models is that its predictions for many universal quantities, including critical exponents, become exact not only for $4-d \ll 1$ but also for $d-2 \ll 1$ (for $N > 2$) (see, for example, [17, 18]) and for any d in the large- N limit [28]. The DE is, at least, an educated interpolation between well-known limits.

Since the original works on NPRG [14, 16] it was argued that the exact equations have a dressed one-loop structure where all propagators are regularized in the infrared, ensuring the smoothness of the vertices as a function of momenta and allowing such an expansion. Moreover, the integral in Eq. (8) – or its derivatives with respect to the fields such as (10) or (11) – includes $\partial_t R_k(q)$ in the numerator, which tends rapidly to zero when $q \gtrsim k$. This implies that the integral over q is dominated by the range $q \lesssim k$. A further progress was made

in Refs. [29, 30] where the regime of validity of this approximation has been discussed. It was observed that an expansion in all momenta (internal and external) gives equations that couple only weakly to the regime of momenta $p \gg k$. Accordingly, it makes sense for these equations to formulate the DE approximation scheme that only applies to the calculation of vertices and its derivatives for momenta that are smaller than k or the smallest mass in the problem. In the case of critical phenomena when $k \rightarrow 0$ the regime of validity of the DE reduces to those quantities dominated by zero momenta (as thermodynamic properties or critical exponents).

The radius of convergence of this expansion depends on the model considered and on the regulating function R_k . However, in models described by Ginzburg-Landau Hamiltonians whose analytical continuation to the Minkowskian space gives unitary models, the radius has been shown to be of the order $q_{radius}^2/k^2 \simeq 4-9$ [19] once an appropriate regulator is chosen with very specific *a priori* criteria. On top of the previous specifications, one needs to fix the scale associated with the normalization of the fields in such a way that all correlation functions at momenta $q^2/k^2 \lesssim 4-9$ behave as in the massive theory. In that case the convergence of the DE takes place as in the massive theory and the dependence on the regulator becomes locally smallest. In practice this requirement is implemented by using a ‘‘Principle of Minimal Sensitivity’’ (PMS) [27, 31] that is explained in detail below.

Given that the integral in (8) [or similarly the integrals for vertex functions such as (10) or (11)] are dominated by internal momenta of order $q \lesssim k$, each successive order in the DE has an error, in low momenta properties of the theory, that is suppressed by a factor $1/9-1/4$. The radius of order 4 to 9 corresponds to the ratio between the square of the smallest mass in the Minkowskian version of the model, and the minimum energy of the 2-particle (or 3-particle) state. If the regulator is chosen properly, the error in the calculation of correlation functions is reduced by a factor $1/9-1/4$ at successive order of the DE.

The quality of most DE results is further improved at low orders because of an independent reason, as explained in Ref. [19]. Consider the 2-point function near the fixed point and define:

$$\gamma_{ab}(p; \phi) = \frac{\Gamma_{ab}^{(2)}(p; \phi) - \Gamma_{ab}^{(2)}(p=0; \phi)}{p^2}. \quad (12)$$

When $p \gg k$ and/or $\phi \gg k^{\frac{d-2+\eta}{2}}$, there is a physical scale that regulates the theory and the regulator can be neglected. As a consequence, in this regime, the function has a scaling behavior and behaves as

$$\gamma_{ab}(p; \phi) \sim p^{-\eta} \hat{\gamma}_{ab} \left(\frac{\phi}{p^{(d-2+\eta)/2}} \right). \quad (13)$$

This means that, in the scaling regime, both the dependence on p and on ϕ are controlled by an exponent of the order of η . By continuity, in the opposite regime $p \lesssim k$,

the function $\gamma_{ab}(p; \phi)$ must show a dependence on p and ϕ of the order of magnitude of η . This means that, for the 2-point function, all corrections to the LPA (where all terms with derivatives are depreciated, except for an unrenormalized term $(\partial\phi)^2$) are suppressed by a factor of η which, in many models, is very small. As a consequence, all quantities that can be extracted from the 2-point function in a uniform magnetic field (such as the exponents η and ν) are already very well estimated at order $\mathcal{O}(\partial^2)$. This makes the convergence very fast in all cases where the exponent η is small. It is important to stress that this *does not* mean that the expansion parameter of the DE is of order η . This factor suppresses all corrections to LPA but does not suppress successive orders of the DE which are only suppressed by a factor $1/9-1/4$.

This analysis is applicable, in particular, in the important \mathbb{Z}_2 and $O(N)$ models with $N \geq 1$. This is consistent with the fact that the DE shows a rapid apparent convergence at low orders for $O(N)$ models. In fact, the DE has been pushed with success to orders $\mathcal{O}(\partial^4)$ [26] and $\mathcal{O}(\partial^6)$ [19] for the Ising universality class, giving excellent results that improve significantly with the order of the DE. Below, it will be shown that the quality of the results extends to all $O(N)$ models at order $\mathcal{O}(\partial^4)$. A mention must be made to the appearance of Goldstone modes in the broken phase of $O(N)$ models for $N \neq 1$. Naively, one could think that the analysis of Ref. [19] does not apply (at least in the low temperature phase) because of the existence of these zero-mass modes. However, the expansion must be done by including the full propagator that includes the regulating function. This gives a square mass of the order of $R_k(0)$ to all modes, including the Goldstone modes. Hence, in the same way as in the regulated theory, the critical regime behaves as a massive theory in the $N = 1$ case and additionally both the critical regime and the low temperature phase behave as massive theories for $k > 0$ (even if the theory presents massless modes when $k \rightarrow 0$).

We indicate here that there exist several exact RG equations, which have different convergence properties in the DE. For example, the Wilson-Polchinski equation [1, 25] involves all 1-Particle Reducible diagrams which generate the connected correlation functions, may they be 1-Particle Irreducible (1PI) or not. This is at odds with NPRG equations where only 1PI diagrams contribute. As a consequence, the radius of convergence is of order $q^2/k^2 \sim 1$. This implies that the DE for the Wilson-Polchinski flow has a control parameter of order one, which explains why the DE gives much better results in the NPRG formulation [17], even at order $\mathcal{O}(\partial^2)$, than in the Wilson-Polchinski's one [32] (as had also been observed in perturbation theory [33]).

In the present work we will analyze only critical exponents (that are universal). We can therefore use as microscopic action a simple Ginzburg-Landau model with

Hamiltonian or Euclidean Action,

$$S[\phi] = \int_x \left\{ \frac{1}{2} (\partial_\mu \phi^a)^2 + \frac{r}{2} \phi^a \phi^a + \frac{u}{4!} (\phi^a \phi^a)^2 \right\}. \quad (14)$$

In order to implement the DE, one considers, at each order of the approximation, the most general terms compatible with the symmetries of a given universality class with a limited number of derivatives. In the case of the critical regime of $O(N)$ models, we require invariance under space isometries and under the internal $O(N)$ symmetry. To be explicit, in the $O(N)$ model, the lowest orders approximations are:

- The Local Potential Approximation (LPA) or order $\mathcal{O}(\partial^0)$ which consist in taking no derivative of the field except a bare, unrenormalized, kinetic term:

$$\Gamma_k^{\partial^0}[\phi] = \int_x \left\{ U_k(\rho) + \frac{1}{2} (\partial_\mu \phi^a)^2 \right\}. \quad (15)$$

Here, the running effective potential $U_k(\rho)$ is an arbitrary function of $\rho = \phi_a \phi_a / 2$.

- The $\mathcal{O}(\partial^2)$, which is the next-to-leading order, consists in taking all the possible terms compatible with the symmetries of the model and with at most two derivatives. In this case the *ansatz* reads:

$$\Gamma_k^{\partial^2}[\phi] = \int_x \left\{ U_k(\rho) + \frac{1}{2} Z_k(\rho) (\partial_\mu \phi^a)^2 + \frac{1}{4} Y_k(\rho) (\partial_\mu \rho)^2 \right\}. \quad (16)$$

For $N = 1$ the terms in $Z_k(\rho)$ and $Y_k(\rho)$ are equivalent and, accordingly, only the $Z_k(\rho)$ function is included.

- Along the same lines, the order $\mathcal{O}(\partial^4)$, which is the next-to-next-to-leading order, gives rise to the *ansatz*:

$$\begin{aligned} \Gamma_k^{\partial^4}[\phi] = & \int_x \left\{ U_k(\rho) + \frac{1}{2} Z_k(\rho) (\partial_\mu \phi^a)^2 + \frac{1}{4} Y_k(\rho) (\partial_\mu \rho)^2 \right. \\ & + \frac{W_1(\rho)}{2} (\partial_\mu \partial_\nu \phi^a)^2 + \frac{W_2(\rho)}{2} (\phi^a \partial_\mu \partial_\nu \phi^a)^2 \\ & + W_3(\rho) \partial_\mu \rho \partial_\nu \phi^a \partial_\mu \partial_\nu \phi^a + \frac{W_4(\rho)}{2} \phi^b \partial_\mu \phi^a \partial_\nu \phi^a \partial_\mu \partial_\nu \phi^b \\ & + \frac{W_5(\rho)}{2} \varphi^a \partial_\mu \rho \partial_\nu \rho \partial_\mu \partial_\nu \varphi^a + \frac{W_6(\rho)}{4} \left((\partial_\mu \varphi^a)^2 \right)^2 \\ & + \frac{W_7(\rho)}{4} (\partial_\mu \phi^a \partial_\nu \phi^a)^2 + \frac{W_8(\rho)}{2} \partial_\mu \phi^a \partial_\nu \varphi^a \partial_\mu \rho \partial_\nu \rho \\ & \left. + \frac{W_9(\rho)}{2} (\partial_\mu \varphi^a)^2 (\partial_\nu \rho)^2 + \frac{W_{10}(\rho)}{4} \left((\partial_\mu \rho)^2 \right)^2 \right\}. \quad (17) \end{aligned}$$

As for the order $\mathcal{O}(\partial^2)$, there are many terms in the $O(N)$ case at order $\mathcal{O}(\partial^4)$ that are identical in the \mathbb{Z}_2 case. Indeed, in the \mathbb{Z}_2 case there are only three independent terms [26] (see below) with four derivatives.

- The order $\mathcal{O}(\partial^6)$ has only been analyzed in the \mathbb{Z}_2 universality class [19]. In that case, the *ansatz* for $\Gamma_k[\phi]$

reads:

$$\begin{aligned} \Gamma_k^{\partial^6, \mathbb{Z}^2}[\phi] = \int_x \left\{ U_k(\phi) + \frac{1}{2} Z_k(\phi) (\partial_\mu \phi)^2 \right. \\ + \frac{1}{2} W_k^a(\phi) (\partial_\mu \partial_\nu \phi)^2 + \frac{1}{2} \phi W_k^b(\phi) (\partial^2 \phi) (\partial_\mu \phi)^2 \\ + \frac{1}{2} W_k^c(\phi) ((\partial_\mu \phi)^2)^2 + \frac{1}{2} \tilde{X}_k^a(\phi) (\partial_\mu \partial_\nu \partial_\rho \phi)^2 \\ + \frac{1}{2} \phi \tilde{X}_k^b(\phi) (\partial_\mu \partial_\nu \phi) (\partial_\nu \partial_\rho \phi) (\partial_\mu \partial_\rho \phi) \\ + \frac{1}{2} \phi \tilde{X}_k^c(\phi) (\partial^2 \phi)^3 + \frac{1}{2} \tilde{X}_k^d(\phi) (\partial^2 \phi)^2 (\partial_\mu \phi)^2 \\ + \frac{1}{2} \tilde{X}_k^e(\phi) (\partial_\nu \phi)^2 (\partial_\mu \phi) (\partial^2 \partial_\mu \phi) + \frac{1}{2} \tilde{X}_k^f(\phi) (\partial_\rho \phi)^2 (\partial_\mu \partial_\nu \phi)^2 \\ \left. + \frac{1}{2} \phi \tilde{X}_k^g(\phi) (\partial^2 \phi) ((\partial_\mu \phi)^2)^2 + \frac{1}{96} \tilde{X}_k^h(\phi) ((\partial_\mu \phi)^2)^3 \right\}. \quad (18) \end{aligned}$$

For $O(N)$ models at order $\mathcal{O}(\partial^6)$, instead of eight independent functions $X^i(\rho)$ corresponding to terms with six derivatives as in the $N = 1$ case, one must introduce 48 independent functions of ρ whose treatment would be a formidable task.

At a given order of the DE, the flow of the various functions is obtained by inserting the corresponding *ansatz* in Eq. (8) and expanding and truncating the right-hand-side on the same functional subspace. For instance, in order to deduce the equation for the effective potential at order $\mathcal{O}(\partial^2)$ one must insert in the exact equation (10) the propagator obtained from the 2-point vertex extracted from the *ansatz* (16):

$$\begin{aligned} \Gamma_{ab}^{(2)}(p; \phi) = \delta_{ab} (U'_k(\rho) + Z(\rho) p^2) \\ + \phi_a \phi_b (U''_k(\rho) + \frac{1}{2} Y(\rho) p^2) + \mathcal{O}(p^4), \quad (19) \end{aligned}$$

As for the potential, the equation for $Z_k(\rho)$ or $Y_k(\rho)$ can be obtained from the equation for the 2-point function in a uniform external field. In order to do so, one must express those functions in terms of the vertices (or its derivatives) in a uniform field. For example,

$$Z_k(\rho) = \frac{1}{N-1} \left(\delta_{ab} - \frac{\phi_a \phi_b}{2\rho} \right) \partial_{p^2} \Gamma_{ab}^{(2)}(p; \phi) |_{\mathbf{p}=0}. \quad (20)$$

It is obvious from the previous expression that the $N = 1$ case must be treated separately. This is a manifestation of the fact that for $N = 1$ the terms in the effective action including $Z(\rho)$ and $Y(\rho)$ are different representations of an identical term. A similar procedure can be implemented at any order of the DE.

The flow equations for the various functions have been obtained in the past at order $\mathcal{O}(\partial^2)$ (see, for example, [34]) and, for $N = 1$, at order $\mathcal{O}(\partial^4)$ [19, 26]. We obtained our equations for arbitrary N at order $\mathcal{O}(\partial^4)$ by implementing a Mathematica code. We verified that our equations reduce to previously known $\mathcal{O}(\partial^2)$ equations when $\mathcal{O}(\partial^4)$ terms are neglected. We also verified that we recovered previous $\mathcal{O}(\partial^4)$ results for $N = 1$ in the corresponding limit. We point out that in this work, like in the previous $\mathcal{O}(\partial^6)$ work of [19], we implement in the flow equations a strict polynomial expansion in momenta at the considered order of the DE. For instance, one of

the contributions to the flow of $\Gamma^{(2)}(p)$ at order $\mathcal{O}(\partial^4)$ involves the product of two $\Gamma^{(3)}$ functions, see Eq. (11). At this order of the DE, these two functions are polynomials of order 4 in their momenta, and their product therefore involves up to 8 powers of the momenta. In our implementation of the DE at $\mathcal{O}(\partial^4)$, we drop such terms, as well as other terms which contain more than 4 powers of the momenta. This differs from more standard implementations of the DE [26, 34] where all terms are kept in the flows even though many other terms of order 6 and 8 have been neglected². Of course, we use the same procedure for all the flows that we consider. We verified that our Mathematica code recovers properly both versions of the equations. In practice, our implementation of the DE yields much simpler expressions for the flows than those obtained with the standard implementation of the DE. They are moreover probably much better under control numerically at order 4 where the flows of some functions involve the product of four $\Gamma^{(3)}$ functions. The details of the numerical solution of the equations is presented in Appendix B.

At criticality—the regime on which we focus in this article—the system is scale invariant. To reach the critical regime typically requires to fine-tune one bare coupling in the initial condition for the flow equations. The Ward identities for scale invariance in the presence of the infrared regulator ΔS_k are equivalent to a *fixed point* condition on the flow of Γ_k , that is, $\partial_t \Gamma_k = 0$ when it is expressed in terms of dimensionless and renormalized quantities [35]. More precisely, one defines renormalized and dimensionless fields and coordinates by

$$\tilde{x} = kx, \quad (21)$$

$$\phi^a(x) = k^{(d-2)/2} Z_k^{-1/2} \tilde{\phi}^a(\tilde{x}), \quad (22)$$

$$\rho(x) = k^{(d-2)} Z_k^{-1} \tilde{\rho}(\tilde{x}). \quad (23)$$

and functions $\tilde{F}(\tilde{\rho}(\tilde{x}))$:

$$F(\rho) = k^{d_F} Z_k^{n/2} \tilde{F}(\tilde{\rho}) \quad (24)$$

where $F(\rho)$ is any function appearing in the *ansatz* for Γ_k : $U_k(\rho), Z_k(\rho), \dots, W^{10}(\rho), d_F$ is the canonical dimension of F and n the number of fields ϕ^a that multiply F in Γ_k . The field renormalization factor Z_k which appears in previous equations is related to the function $Z_k(\rho)$ in the following way. We first define the renormalized equivalent of $Z_k(\rho)$ by the relation $Z_k(\rho) = Z_k \tilde{Z}_k(\tilde{\rho})$. The renormalization factor \tilde{Z}_k is then defined by the (re)normalization condition: $\tilde{Z}_k(\tilde{\rho}_0) = 1$ for a fixed value of $\tilde{\rho}_0$. The running anomalous dimension η_k is then defined by $\eta_k = -\partial_t \log Z_k$. At the fixed point, it becomes the actual anomalous dimension η [17].

² We verified explicitly that both versions of the DE give results that are compatible within error bars at order $\mathcal{O}(\partial^2)$.

III. REVIEW OF PREVIOUS DERIVATIVE EXPANSION RESULTS FOR THE $N = 1$ CASE

We now consider results in the Ising universality class (corresponding to the $N = 1$ case). This universality class has been studied many times at LPA and order $\mathcal{O}(\partial^2)$ [14, 17, 18, 27, 34, 36–42] and even at order $\mathcal{O}(\partial^4)$ [26]. However, depending on the authors, slightly different flow equations have been considered and in some cases, on top of the DE, the functions $U_k(\phi)$, $Z_k(\phi)$ and $W_k^i(\phi)$ have been replaced by their Taylor expansion in ρ truncated at finite order. In a recent article [19], the order $\mathcal{O}(\partial^6)$ has been analyzed and the critical exponents η and ν were compared to the very precise results coming from the CB [11–13]. This calculation has allowed for a quantitative analysis of the error of the DE up to order 6 and has suggested a methodology to estimate the error bars. We show in detail in Sect. IV how to implement this analysis in the $O(N)$ case. The information obtained for $N = 1$ will be an important guide when estimating error bars in the more general $O(N)$ case. In the present section we review the $N = 1$ results. In Sect. VA we extend them at order $\mathcal{O}(\partial^4)$ for the exponent ω (related to corrections to scaling).

At this point, it is important to stress that the DE — like any approximation scheme — introduces a spurious dependence of the critical exponents on the regulating function R_k mentioned in Sect. IIB. In the DE the role of the regulator is more important than in other approximations because the mere formulation of the approximation *requires* that we have introduced the regulator. That is, the approximation is only justified for momenta smaller than two to three times k , the scale of the regulator. This is at odds with other approximation schemes which do not treat only a limited range of momenta (as, for example, [29, 30, 43]).

For each family of regulators we analyzed the dependence of critical exponents on the regulating function on the overall scale α . For the considered regulators it turns out to be the most important dependence on the regulating function. In order to fix this scale, we use the “Principle of Minimal Sensitivity” (PMS) [27, 31]. The underlying rationale is that, in the exact theory, the exponents do not depend on the overall scale of the regulator, and therefore an optimal choice of α is obtained when the physical results depend least on this parameter. In many cases, the exponents as a function of α present a local extremum and in those cases the α_{PMS} is just the value corresponding to this extremum.

In a second step, one can change the shape of the regulating function and see how the PMS results are spread. In Ref. [19] three families of regulators were employed:

$$W_k(q^2) = \alpha Z_k k^2 y / (\exp(y) - 1) \quad (25a)$$

$$\Theta_k^n(q^2) = \alpha Z_k k^2 (1 - y)^n \theta(1 - y) \quad (25b)$$

$$E_k(q^2) = \alpha Z_k k^2 \exp(-y) \quad (25c)$$

where $y = q^2/k^2$.

The regulator (25a) with $\alpha = 1$ was proposed by Wetterich [14] and the α -dependence of physical quantities such as exponents was studied in [27], [26] and [19]. It turns out that fixing the prefactor by the PMS procedure improves significantly the results of the DE compared to the standard value $\alpha = 1$. Being smooth, the DE can be applied with this regulating function at any order. Another convenient regulator was proposed by Litim [42]. It is non-analytic but smoother than the sharp cut-off [36] commonly employed with the Wilson-Polchinski equations [1, 25] (see below). It corresponds to the Θ_k^n regulator defined in Eq. (25b) with $n = 1$ and $\alpha = 1$. It allows for the analytic calculation of many integrals involved in the LPA flows and there are strong indications that this is the optimal choice at the LPA order [42, 44]. However, since it is non-analytic, it is not well-suited for a systematic expansion in momenta, as is done in the DE. Moreover, it turns out that it is not optimal at order $\mathcal{O}(\partial^2)$ [27] and is incompatible with the DE at order $\mathcal{O}(\partial^4)$ due to the non-analyticities it induces in the flows. At any finite order of the DE, regulators of the family (25b) can be used under the condition that their index n is large enough to keep the flows smooth-enough for the various considered functions to be well-defined. Another smooth regulator used in [19, 45] corresponding to expression (25c) will be considered below. In that case, also, it has been observed that the PMS turns out to be an efficient optimization procedure [19] for $N = 1$ and, as shown below, this is also true for more general $O(N)$ models.

Each regulating function studied in Ref. [19] yielded very similar results once the overall scale α is fixed by the PMS. It must be mentioned, however, that in the literature, other regulators have been also considered giving results of lower quality. In particular, the sharp cut-off was employed by Wegner and Houghton at order LPA [36] long time before the modern implementation of NPRG. The sharp cut-off corresponds to the regulating function

$$S_k(q^2) = \begin{cases} \infty & \text{if } q < k \\ 0 & \text{if } q > k \end{cases} \quad (26)$$

The strong non-analyticities induced by this regulator in the flows do not allow for the implementation of the DE beyond the LPA ³. Power law regulators have also been studied by Morris [39, 40]. They however yield relatively poor results at LPA and $\mathcal{O}(\partial^2)$ probably because of two independent reasons. First, the large momentum region, which is beyond the radius of convergence of the DE, is only suppressed in the integrals involved in the flows as power laws at odds with the regulators (25a), (25b) and (25c). Second, being non-analytic at $q = 0$, the convergence properties of the DE are not controlled by the small parameter discussed before.

³ Let us note, however, that Morris implemented a similar momentum scale expansion [46] for this regulator.

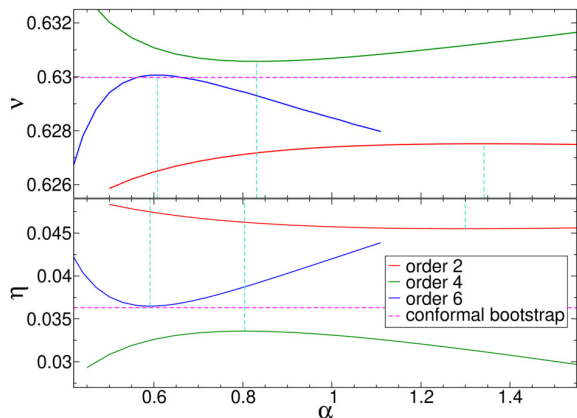


FIG. 1. Dependence of the critical exponents $\nu(\alpha)$ and $\eta(\alpha)$ with the coefficient α for different orders of the DE (figure from Ref. [19]). LPA results do not appear within the narrow ranges of values chosen here (see Table I).

Let us discuss as an example the results obtained in [19] with the regulator (25c). In Fig. 1 (from Ref. [19]) the dependence of the critical exponents $\nu(\alpha)$ and $\eta(\alpha)$ with the coefficient α is represented for different orders of the DE. At each order, the curves for the exponent exhibit a maximum or a minimum at some value α_{PMS} . When increasing the order of the DE, the extrema alternate between being a maximum and a minimum (this is true for both exponents). Following the PMS criteria, the values $\nu(\alpha_{\text{PMS}})$ and $\eta(\alpha_{\text{PMS}})$ can be selected as best estimates. Moreover, given that the concavities of the curves alternate, these results are those that gives the fastest apparent convergence because they reduce the difference between two consecutive orders. At a given order of the DE, $\alpha_{\text{PMS}}^{(\nu)}$ and $\alpha_{\text{PMS}}^{(\eta)}$ are close but different, and their difference decreases with the order of the DE, see Fig. 1.

The values of the exponents at α_{PMS} converge very fast to values very close to the CB quasi-exact ones. In most cases they also alternate around these values. The only exception is at order $\mathcal{O}(\partial^6)$. At this order, the optimal value of ν ‘crosses’ the CB values, but at this order PMS results coincide with CB values up to three or four significant digits, see Fig. 1 and Table I. It is possible that this property is exact for correlation functions [as seen for $N = 1$ up to order $\mathcal{O}(\partial^6)$ [19]] but is only an approximation for critical exponents that are not directly related to a single correlation function. Surprisingly, the local curvature at α_{PMS} increases with the order of the DE. That could indicate that for generic values of α the convergence of the DE could be doubtful but, at PMS, the exponents seem to converge to the best estimates in the literature. The increase of curvature at α_{PMS} and the accompanying faster variations of exponent values with α when increasing the order of the DE imply that it is crucial to work with the optimal values given by the PMS criteria, that is $\nu(\alpha_{\text{PMS}}^{(\nu)})$ and $\eta(\alpha_{\text{PMS}}^{(\eta)})$.

TABLE I. Raw results of the DE from various previous references for the Ising critical exponents ν and η in $d = 3$ obtained with various regulators. When a value of α different from PMS is employed, this is explicitly indicated. The numbers in parentheses for DE results give the distance of the results to the CB [13] values given here as the almost exact reference.

	regulator	ν	η
LPA	W [19, 27]	0.65059(2062)	0
	Θ^1 [42]	0.64956(1956)	0
	Θ^3 [19]	0.65003(2006)	0
	Θ^4 [19]	0.65020(2023)	0
	Θ^8 [19]	0.65056(2059)	0
	E [19]	0.65103(2106)	0
	E [19]	0.65103(2106)	0
	Power-law [40]	0.66	0
	S [37]	0.687	0
$\mathcal{O}(\partial^2)$	W [19]	0.62779(218)	0.04500(870)
	W ($\alpha = 1$) [41]	0.6307	0.0467
	Θ^1 [27]	0.6260	0.0470
	Θ^2 [19]	0.62814(183)	0.04428(798)
	Θ^3 [19]	0.62802(195)	0.04454 (824)
	Θ^4 [19]	0.62793(204)	0.04474(844)
	Θ^8 [19]	0.62775(222)	0.04509(879)
	E [19]	0.62752(245)	0.04551(921)
	Power-law [40]	0.618	0.054
$\mathcal{O}(\partial^4)$	W [19]	0.63027(30)	0.03454(176)
	W (field expansion)[26]	0.632	0.033
	Θ^3 [19]	0.63014(17)	0.03507(123)
	Θ^4 [19]	0.63021(24)	0.03480(150)
	Θ^8 [19]	0.63036(39)	0.03426(204)
	E [19]	0.63057(60)	0.03357(272)
	$\mathcal{O}(\partial^6)$	W [19]	0.63017(20)
Θ^4 [19]		0.63013(16)	0.03591(39)
Θ^8 [19]		0.63012(15)	0.03610(20)
E [19]		0.63007(10)	0.03648(18)
CB [13]		0.629971(4)	0.0362978(20)

Once the parameter α is fixed with the PMS procedure, the speed of convergence is in agreement with the considerations about the radius of convergence of the DE at criticality. That is, the amplitude of the oscillations of the optimal values considered as functions of the order of the DE decreases typically by a factor that is consistent with the convergence estimate at each successive order (4 to 9, see Table I). Moreover, for each exponent, the dispersion of values (over all regulators studied) typically also decreases by similar factors when going from one order to the next. This can also be interpreted as a manifestation of the radius of convergence of the DE, see Table I.

After a rather extensive exploration of different regulators, the authors of [19] have conjectured the existence,

for a given exponent and a given order of the DE, of an absolute extremum value, (an absolute maximum or an absolute minimum, depending on the exponent and the order considered) that cannot be passed by any regulator. As we discuss below, this general conjecture seems not to be fulfilled for all $O(N)$ models and all exponents. However, in many important cases, at least up to order $\mathcal{O}(\partial^4)$ and for exponents ν and η , it seems to be correct. We discuss this point in the next section and explain how it can be used to improve the estimate of critical exponents.

IV. EXPANSION PARAMETER AND ERROR BARS

In the present section, we exploit the existence of a small expansion parameter in the DE of $O(N)$ models to estimate the error bars for various critical exponents. As explained in Ref. [19] and reviewed in the previous sections, when calculating vertex functions or their derivatives at zero momenta, the DE is controlled by a small parameter of order $1/9-1/4$. This leads to a well-grounded estimate of error bars that can be employed in general models. We discuss and implement them concretely below both for the Ising universality class and for general $O(N)$ models.

A. A first estimate of error bars

Let us first discuss a generic estimate of error bars within the DE (at least for models where there is a unitary Minkowskian extension). Consider a physical quantity Q that we aim at computing. The procedure is simple:

- For a given regulator family and at a given order of the DE, we choose as value of Q the one corresponding to the α determined by PMS procedure.
- When comparing among different families of regulating functions, without further information, it is reasonable to choose the value at the center of the range of values for Q obtained for the considered regulators. Let us call $\bar{Q}^{(s)}$ this estimate at order $\mathcal{O}(\partial^s)$.
- Having determined the estimates $\bar{Q}^{(s)}$ at various orders, we choose as first error estimate at order $\mathcal{O}(\partial^s)$, $\Delta Q^{(s)} = |\bar{Q}^{(s)} - \bar{Q}^{(s-2)}|/4$. The $1/4$ corresponds to the more conservative estimation of the small parameter. Indeed, dividing by four in many cases turns out to be a pessimistic choice. Nevertheless, without further information, it is convenient to choose pessimistic error bars.

Observe that this procedure does not lead to an estimate of error bars at order LPA because it requires at least two

consecutive orders. It is also interesting to observe that it can be employed for any physical observable (which can be extracted from a vertex or its derivatives at zero momenta). In Table II the results of the present analysis are presented for the exponents ν and η in the Ising universality class given in Ref. [19]. Comparing with the results of the CB, one observes that the DE estimates seem to converge to the quasi-exact values and that estimated error bars are correct (or, more precisely, somewhat pessimistic).

On top of these estimates of error bars, it is necessary to take into account the dependence of the results among the various families of regulators which is an independent source of errors (in most cases much smaller than the one that we just considered). Moreover, we should have in mind that these estimates are typically pessimistic but can become too optimistic in the exceptional case where two consecutive orders of the DE accidentally cross. This possibility can be avoided by considering a more typical (and pessimistic) estimate in the case of exceptional “crossings”. We discuss these independent sources of error in Sect. IV C.

Before considering this point, it is important to stress that given our knowledge of the actual behavior of exponents at the various orders in the Ising universality class, one can test in this case the quality of the proposed estimate of error bars. This information can be used to improve the estimate of central values and error bars as explained in the next subsection. This will be exploited in Sect. V in the analysis of other $O(N)$ models at order $\mathcal{O}(\partial^4)$.

B. Improving the estimate of central values and error bars

As explained in the previous section, in most cases the concavity of the curve of exponents as a function of α alternates. Moreover, the results obtained at a given order of the DE do not intersect with the previous one. As a consequence, in those cases, choosing the PMS also leads to the fastest apparent convergence by reducing the difference of critical exponents estimates in consecutive orders. In those cases we also have strong reasons to believe that, up to that order, the DE gives alternating bounds (upper or lower) of critical exponents. As a consequence, the estimate $\bar{Q}^{(s)}$ is clearly not the optimal choice and the extremum among the values obtained via PMS for various reasonable regulators seem to be a much more reasonable estimate. Let us call this extremum $Q_{ext}^{(s)}$.

Note, however, that this estimate does not fully exploit the information that DE expansion, in those cases, are bounds. One then expects the exponent to lie in-between the results obtained in two consecutive orders of the DE. For example, for the $N = 1$ exponent ν at order $\mathcal{O}(\partial^4)$ one would expect that the actual value of the exponent lies in the interval $[\nu_{ext}^{(2)}, \nu_{ext}^{(4)}]$. The value $\nu_{ext}^{(4)} = 0.63014$ is not an optimal estimate of the exponent at that or-

TABLE II. Analysis of error bars at orders $\mathcal{O}(\partial^0)$ (LPA) to $\mathcal{O}(\partial^6)$. Raw data extracted of [19]. See text for the precise definitions of various possible central values and error bars. CB [13] values are also given for comparison.

D.E.	$\bar{\nu}$	$\tilde{\Delta}\nu$	$\tilde{\nu}$	$\tilde{\tilde{\Delta}}\nu$	$\Delta_{reg}\nu$	$\Delta\nu$	$\bar{\eta}$	$\tilde{\Delta}\eta$	$\tilde{\eta}$	$\tilde{\tilde{\Delta}}\eta$	$\Delta_{reg}\eta$	$\Delta\eta$
LPA	0.65030	–	0.64956	–	0.00147	–	0	–	0	–	0	–
$\mathcal{O}(\partial^2)$	0.62783	0.00562	0.63082	0.00268	0.00062	0.00268	0.04490	0.01122	0.03875	0.00554	0.00123	0.00554
$\mathcal{O}(\partial^4)$	0.63036	0.00063	0.62989	0.00025	0.00043	0.00025	0.03432	0.00264	0.03622	0.00115	0.00150	0.00115
$\mathcal{O}(\partial^6)$	0.63012	0.00006	–	–	0.00010	0.00016	0.03615	0.00046	0.03597	0.00018	0.00067	0.00113
CB	0.629971(4)						0.0362978(20)					

der because it is in the border of the interval of expected values. Moreover, given the fact that two consecutive orders give alternating errors that are reduced by a factor $1/9-1/4$, one expects the actual value of the exponent to be closer to $\nu_{ext}^{(4)}$ than to $\nu_{ext}^{(2)}$. Taking into account these considerations, when the values $Q_{ext}^{(s)}$ for some quantity are expected to be extrema, an improved estimate corresponds to shifting $Q_{ext}^{(s)}$ towards the center of interval between $Q_{ext}^{(s)}$ and $Q_{ext}^{(s-2)}$ by $|Q_{ext}^{(s)} - Q_{ext}^{(s-2)}|/8$ and consider as error estimate $\tilde{\Delta}Q^{(s)} = |Q_{ext}^{(s)} - Q_{ext}^{(s-2)}|/8$ ⁴. This new estimate of central value will be called $\tilde{Q}^{(s)}$ and its explicit expression is:

$$\tilde{Q}^{(s)} = \frac{1}{8} \left(7 Q_{ext}^{(s)} + Q_{ext}^{(s-2)} \right) \quad (27)$$

For example, in the same example as before, it is reasonable to give as estimate of ν at order $\mathcal{O}(\partial^4)$ the following improved estimate of central values and error bars:

$$\begin{aligned} \tilde{\nu}^{(4)} &= \nu_{ext}^{(4)} - |\nu_{ext}^{(2)} - \nu_{ext}^{(4)}|/8 = 0.62989 \\ \tilde{\tilde{\Delta}}\nu^{(4)} &= |\nu_{ext}^{(2)} - \nu_{ext}^{(4)}|/8 = 0.00025 \end{aligned} \quad (28)$$

These improved estimates are reasonable (see Table II) as long as we have strong reasons to believe that the DE gives, at this order, a bound for the considered physical quantity Q . A necessary condition for this is that two consecutive orders of the DE give results for the various families of regulators that are disjoint and that, for any regulator, the considered quantity represented as a function of α shows the appropriate convexity. Among the results obtained for $N = 1$ there is a single exception. The results of orders $\mathcal{O}(\partial^4)$ and $\mathcal{O}(\partial^6)$ overlap for the exponent ν : the ν exponent obtained with regulator W at order $\mathcal{O}(\partial^6)$ is larger than the one obtained with regulator Θ^3 at order $\mathcal{O}(\partial^4)$ (see Table I). In that case, it makes no sense anymore to choose as optimal value the extremum among regulators because the precision of the DE has reached a point where exponents coming from

the various families of regulators spread around the exact value. When an overlap between two consecutive orders have been reached, there is no reason to expect that the results represent bounds for a given quantity and it is necessary to go back to the estimate $Q^{(s)}$ described in Sect. IV A. More generally, without a strong reason supporting that a certain order of the DE gives bounds on a certain physical quantity, it is safer to use the previously presented more conservative central value and error bar. As an example, for the exponent η there is no broad empirical experience or theoretical information that could lead us to think that the order $\mathcal{O}(\partial^6)$ gives a bound for the exponent (except from an extrapolation of the behavior at previous orders)⁵. At order $\mathcal{O}(\partial^6)$ a single model has been studied and only two exponents have been calculated. This does not give us enough experience to use improved estimates of central values and error bars but it does give us a good control of the *previous* order $\mathcal{O}(\partial^4)$ that we can exploit when studying the $O(N)$ models.

In the case of $O(N)$ models up to order $\mathcal{O}(\partial^4)$ there are strong indications that the raw results for the considered exponents coming from the DE are, in many cases, bounds for the actual values for ν and η and, accordingly, we will consider the improved estimate of exponents in those cases. This seems clearly to be the case for η for all values of N and for ν for moderate values of N , at least for $1 \leq N \leq 5$. It is important, however, to point out that in non-unitary cases ($N = 0$ and $N = -2$) that we analyze in Sect. V E, the DE does not seem to show consistent bounds on the exponents for η and ν . In the same way, when N is large ($N \gtrsim 10$), there are indications that the DE expansion does not give bounds for the exponent ν . Let us note, however, that the dependence on the regulator becomes very small when N grows, making the optimization of the regulator a much less relevant issue in that limit.

The case of exponent ω is different. As explained below the estimates of various orders of the DE for this exponent do not seem to correspond to bounds in any

⁴ For a radius of convergence a , we would shift by $|Q_{ext}^{(s)} - Q_{ext}^{(s-2)}|/(2a)$. We choose the most conservative radius of convergence $a = 4$.

⁵ In fact, $\mathcal{O}(\partial^6)$ does not give a bound on this exponent but we only know that by exploiting the good estimates obtained for this exponent by other means. In any case when we have no strong reasons for assuming that results are bounds, the more pessimistic estimate should be used.

particular domain of N . For this exponent we employ the more conservative estimate of central values and errors presented in Sect. IV A. It is interesting to note that even the concavities of the curves of ω as a function of α changes for $N \sim 1$ (see Fig. 2 and Figs. 3 and 6 below).

C. Other sources of error

In this section we analyze two other sources of error to be taken into account.

First, in the previous analysis, only the error associated with the distance between some central value and the exact value coming from the systematic error of the DE has been considered. However, in the cases where the improvement presented in Sect. IV B can not be considered, one must add a further source of uncertainty. That is, when considering various families of regulators, we made the choice of the center of the interval of studied families of regulators but there is no definite reason to take one value or the other. As an estimate of error coming from the uncertainty due to the dependence on the family of regulators, we choose for any quantity Q the distance between the two extreme values obtained among the families of regulators considered and we call it $\Delta_{reg}Q$. This source of uncertainty in most studied cases is much smaller than the one coming from the difference between one order of the DE and the following. However, it turns out that at order $\mathcal{O}(\partial^6)$, one can not neglect it. In all cases that we choose the non-optimized central value Q we will choose as error bar $\Delta Q = \Delta_{reg}Q + \hat{\Delta}Q$ (see Table II).

We now analyze a second possible source of error. When the estimates coming from the DE are not bounds on a given quantity Q it may happen that the estimates of two consecutive orders of the DE cross when we vary some parameter, such as the space dimension d or the number of components of the field N ⁶. In those cases, the error estimate presented in Sect. IV A is no longer appropriate because the difference between two consecutive orders is accidentally small (see Ref. [47] where the same phenomena takes place for other exponents). In that case, it is more convenient to use a typical value of the error bars and not a particular value which is near the “crossing”. This difficulty is encountered in practice for the exponent ω at order $\mathcal{O}(\partial^2)$ because the values for this exponent at that order crosses those of the LPA for N between 3 and 4 (as explained in detail in Sect. V C). To avoid such difficulty, we exploit the fact that the exponent ω becomes exact in the large- N limit. As such, we impose the error to be, at each order of the DE, a monotonically decreasing function of N . This avoids the artificial reduction of error bars for $N = 3, 4$

and 5. Of course, this can give a pessimistic error bar but, as stated before, it is preferable to use conservative error bars than the opposite. A similar difficulty takes place at order $\mathcal{O}(\partial^4)$ for ω because the results from $\mathcal{O}(\partial^2)$ and $\mathcal{O}(\partial^4)$ cross around $N \sim 2$. In that case, however, one can exploit the error bars calculated at order $\mathcal{O}(\partial^2)$ to estimate a very conservative error bars at order $\mathcal{O}(\partial^4)$ without needing to assume a monotonic behavior of error bars. In order to do so, we adopted the following criterion: whenever the estimated error for ω at order $\mathcal{O}(\partial^4)$ is smaller than the error calculated at order $\mathcal{O}(\partial^2)$ divided by four, we adopt this last expression. Doing so, we exclude abnormally small estimates of error bars due to the crossing. In practice, this augment is advocated when evaluating error estimates for $N = 0, 1$ and 2.

V. CRITICAL EXPONENTS FOR $O(N)$ MODELS: DERIVATIVE EXPANSION RESULTS

In the present section we extend previous results to $O(N)$ models at order $\mathcal{O}(\partial^4)$ of the DE. We first compute the correction to scaling exponent ω for $N = 1$, which was not studied previously at this order. We then analyze other values of N and compute the leading exponents η and ν and the correction to scaling exponent ω .

Before considering each particular value of N , it is worth mentioning that the nature of error bars are different in the various studies. CB are able (in many cases) to give rigorous bounds on the values of critical exponents, under mild assumptions on the spectrum of operators for unitary theories. When quoting CB results we employed for all positive values of N such rigorous bounds when available for exponents η and ν . In the case $N = 0$ and for ω most results in the literature within the CB do not have the same level of rigor. In those cases, we should keep in mind that error bars do not have the same meaning as for exponents η and ν in unitary models. In MC studies, statistical error bars are well under control but have a probabilistic interpretation. Other systematic sources of error are much more difficult to handle but for the quoted MC studies, they seem to be under control and consistent with other estimates. For perturbation theory, high-temperature expansion and DE results, the error bars do not have the same level of rigor. They depend on assumptions and on semi-empirical analysis of the results at various orders. Other estimates of various methods seem to give consistent results but we observe that some perturbative error bars seem to be too optimistic because the state-of-the-art results are not within their uncertainty range. This is the case, for example, for the recent ϵ^6 results of Ref. [48] where the resummation technique and the methodology to determine error bars is presented in great detail. However, some of their results are incompatible with the most precise results of the literature. The authors of ref [48] mention this point but they suggest that it is too soon to know if the discrepancies of ϵ^6 results with most precise estimates is

⁶ This difficulty can not take place in the “improved” version because in that case, successive orders are disjoint.

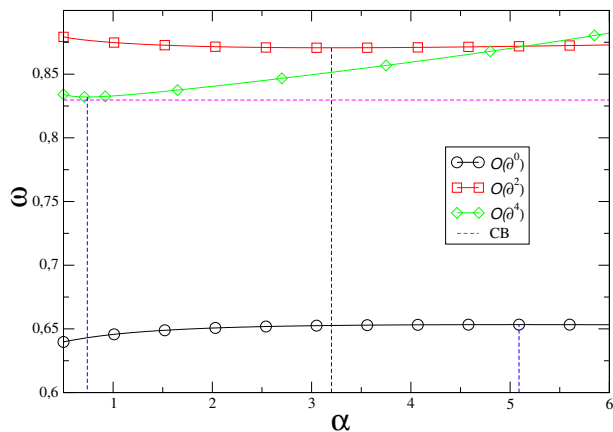


FIG. 2. Exponent ω as a function of α for $N = 1$ for the regulating function (25c).

significant or not and they suggest to wait to ϵ^7 results in order to decide.

In the present study, error bars are to be understood as a bracketing of the exact values. For all critical exponents and values of N that we have considered, we obtain results that are compatible, within error bars, with the most precise estimates in the literature (whenever a prediction more precise than ours is available). The only exception is the value of ω for $N = 100$ at order $O(\partial^4)$ of DE. In this case, it may be that we underestimate the error bars [from our $O(\partial^4)$ result or from large- N expansion]. Even in that case, error bands almost overlap.

A. Results for critical exponents for $N = 1$

Let us consider first the raw data for the correction to scaling exponent ω that can be seen in Table III. In the present work we focus on the regulators that were analyzed in Ref. [19], that can be employed at order $O(\partial^4)$. When $N = 1$, as for the case of η and ν , the raw data for the critical exponent ω gives PMS results at successive orders of the DE [up to order $O(\partial^4)$] which are disjoint. However, as seen in Fig. 2, both $O(\partial^2)$ and $O(\partial^4)$ curves present a minimum, which indicates that the various orders of the DE are not bounds on this critical exponent. The same behavior was observed for other regulators. As a consequence, we use for this exponent the non-improved estimate of central values and errors presented in Sect. IV A. We observe, nevertheless, a very fast convergence achieving a precision of the same order of MC estimates, but as for most other methods in the literature, we have a larger error bar than for leading exponents ν and η .

Before considering other values of N let us sum up the results obtained up to now for the three dimensional Ising universality class, presented in Table IV. It is worth mentioning that the results are very precise (particularly for ν and ω). At first sight one could get the impression

TABLE III. Raw data for $N = 1$ of the critical exponent ω in $d = 3$ obtained with various families of regulators at various orders of the DE. The results are also compared to previous results of the DE. When a value of α different of PMS is employed, this is explicitly indicated. The results of the CB [49] are given for comparison.

	regulator	ω
LPA	W	0.6541
	Θ^1 [42]	0.6557
	Θ^3	0.6551
	E	0.6533
	Power-law [40]	0.63
	S [37]	0.595
$O(\partial^2)$	W	0.8702
	Θ^3	0.8698
	E	0.8707
	Power-law [40]	0.897
$O(\partial^4)$	W	0.8313
	Θ^3	0.8310
	E	0.8321
CB [49]		0.82968(23)

that the order $O(\partial^6)$ does not improve the results significantly with respect to order $O(\partial^4)$ for η and ν . However, this only reflects our poorer experience on the behavior of the DE at order $O(\partial^6)$ and the consequent use of a much more pessimistic estimate of central values and error bars. In fact, by looking directly at the raw data presented in Table I one observes that the DE does give better estimates for any regulator at successive orders, including order $O(\partial^6)$.

Another strategy in order to estimate central values followed in Ref. [19] is to exploit the whole series of data for a given exponent in order to extrapolate the central value and error bars. This strategy gives better estimates of central values and a smaller error bar. However, we follow here a strategy that can be implemented for $O(N)$ models where we only have at our disposal the results for the DE up to order $O(\partial^4)$. More generally, we propose a general method that can be employed safely for very general models where, in most cases, the DE has only been studied up to order $O(\partial^2)$.

B. The controversial $N = 2$ case: the Derivative Expansion take

The $N = 2$ case describes the important XY universality class that corresponds to many physical systems, including easy planes magnetic systems and the λ -transition of the Helium-4 superfluid. For a classical review of various systems in this universality class, we refer to [3]. The $O(2)$ case is particularly important because, as discussed in the Introduction, there is a long-

TABLE IV. Final results at various orders of the DE with appropriate error bars for $N = 1$ in $d = 3$. Results for η and ν are taken from [19]. Results of the CB ([13] for η and ν and [49] for ω), MC [7], High-temperature expansion [50], and 6-loop, $d = 3$ perturbative RG values [2], and ϵ -expansion at order ϵ^5 [2] and at order ϵ^6 [48] are also given for comparison.

	ν	η	ω
LPA	0.64956	0	0.654
$O(\partial^2)$	0.6308(27)	0.0387(55)	0.870(55)
$O(\partial^4)$	0.62989(25)	0.0362(12)	0.832(14)
$O(\partial^6)$	0.63012(16)	0.0361(11)	
CB	0.629971(4)	0.0362978(20)	0.82968(23)
6-loop, $d = 3$	0.6304(13)	0.0335(25)	0.799(11)
ϵ -expansion, ϵ^5	0.6290(25)	0.0360(50)	0.814(18)
ϵ -expansion, ϵ^6	0.6292(5)	0.0362(6)	0.820(7)
High-T.	0.63012(16)	0.03639(15)	0.83(5)
MC	0.63002(10)	0.03627(10)	0.832(6)

standing controversy concerning the value of the critical exponent ν between the most precise experiments⁷ [23] and the best theoretical estimates given by some MC simulations [51, 52] and very recent CB results [24]. Most field-theoretical methods [2, 53] (including CB before [24]) have been unable to decide the point because of the high level of precision reached by experiments and simulations. Indeed, as discussed in [52], there is even a discrepancy among various MC results that in some cases give results compatible with experiments [54], but a consensus seems to have been reached that the most precise simulations [8, 51, 52] are very far away from the experimental prediction. We present now our $O(\partial^4)$ DE estimate of critical exponents η , ν and ω .

The raw data for these exponents obtained at successive orders of the DE for the same regulators mentioned in previous section are presented in Table XVI in Appendix A. We also included in this table the previous results obtained with the DE. As for $N = 1$, for all considered families of regulators the concavity of the curves of exponents η and ν as a function of the parameter α alternates, see Fig. 3. Moreover, the results at successive orders of the DE are disjoint, which strongly indicates alternating bounds on the critical exponents at this order of the DE. Accordingly, we employ the improved estimate of central values and error bars presented in Sect. IV B for those exponents. The corresponding results are presented in Table V where they are compared to other results in the literature both theoretical and experimental. Special attention must be given to the exponent ω where it is seen in Fig. 3 that the results at order (∂^2) and (∂^4) intersect. Moreover, the LPA curve, which is below the

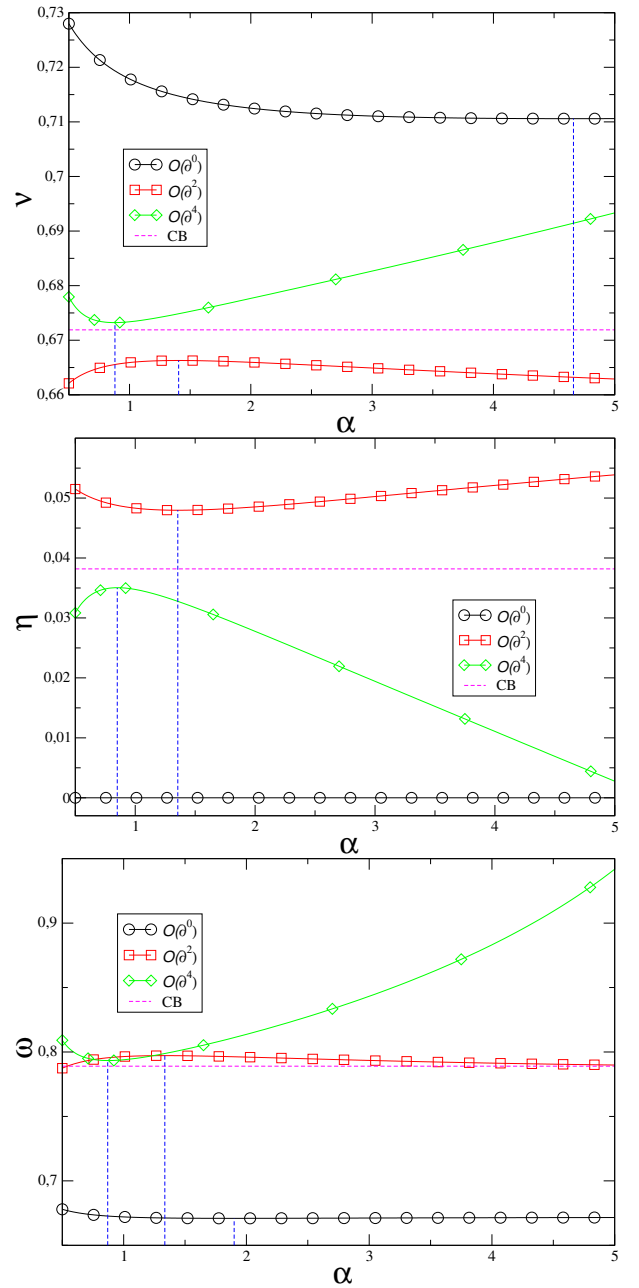


FIG. 3. From top to bottom: exponents ν , η and ω as a function of α for $N = 2$ for the regulating function (25c).

$O(\partial^2)$ one, presents a minimum, not a maximum. The various orders of the DE definitely do not give bounds on that exponent. We therefore use for this exponent the more conservative estimate of error bars described in Sect. IV A. In what concerns ω , we shall use the same pessimistic error bar for other values of N .

We reach for the three exponents very precise estimates. In particular, we obtain a better precision than perturbative estimates. We do not reach, however the level of accuracy of MC [8, 51, 52] and (for ν and η) from the CB [24] which appeared during the completion

⁷ Indeed, the critical exponent that is actually measured is the specific heat exponent α for the transition of the superfluid helium 4, that can be related to ν by a hyper-scaling relation.

TABLE V. Final results at various orders of the DE with appropriate error bars for $N = 2$ in $d = 3$. Results to the CB from 2016 ([53] for η and ν and [55] for ω) and also from 2019 [24], combined MC and High-Temperature analysis from [51] and recent (2019) MC from [8], and 6-loop, $d = 3$ perturbative RG values [2], and ϵ -expansion at order ϵ^5 [2] and order ϵ^6 [48] are also given for comparison. Results for most precise experiments are also included: Helium-4 superfluid from [23] and [56] for ν , XY-antiferromagnets (CsMnF₃ from [57] and SmMnO₃ from [58]), and XY-ferromagnets (Gd₂IFe₂ and Gd₂ICo₂ from [59]). Whenever needed, scaling relations are used in order to express results in terms of η and ν .

	ν	η	ω
LPA	0.7090	0	0.672
$O(\partial^2)$	0.6725(52)	0.0410(59)	0.798(34)
$O(\partial^4)$	0.6716(6)	0.0380(13)	0.791(8)
CB (2016)	0.6719(12)	0.0385(7)	0.811(19)
CB (2019)	0.6718(1)	0.03818(4)	0.794(8)
6-loop $d = 3$	0.6703(15)	0.0354(25)	0.789(11)
ϵ -expansion, ϵ^5	0.6680(35)	0.0380(50)	0.802(18)
ϵ -expansion, ϵ^6	0.6690(10)	0.0380(6)	0.804(3)
MC+High-T. (2006)	0.6717(1)	0.0381(2)	0.785(20)
MC (2019)	0.67169(7)	0.03810(8)	0.789(4)
Helium-4 (2003)	0.6709(1)		
Helium-4 (1984)	0.6717(4)		
XY-AF (CsMnF ₃)	0.6710(7)		
XY-AF (SmMnO ₃)	0.6710(3)		
XY-F (Gd ₂ IFe ₂)	0.671(24)	0.034(47)	
XY-F (Gd ₂ ICo ₂)	0.668(24)	0.032(47)	

of this work. We find, for the controversial value of ν , a result that turns out to be compatible with the most precise MC simulations and CB and incompatible with experiments from [23].

MC and CB clearly give more precise determinations of the critical exponents. We would like to mention, however, that the numerical effort is much bigger in these two methods than the one we had to face. Typically, finding a fixed point takes about 2 hours in a laptop while MC involved several years of CPU time and CB about 10² years of CPU time.

C. Results for some physically interesting cases

We present now result for two other physically relevant cases with positive integer values of N (and, as such, unitary). These are the Heisenberg universality class $N = 3$, relevant for isotropic ferromagnets, and the $N = 4$ universality class relevant for the chiral phase transition in the physics of strong interactions. We refer to [3] for a detailed description of various systems in these two universality classes.

We present now our results at successive orders of the

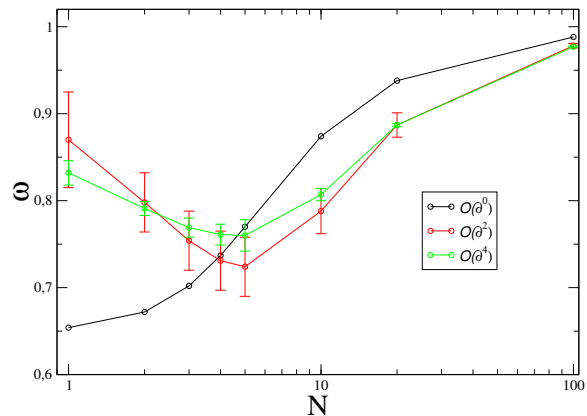


FIG. 4. Exponent ω as a function of $1/N$ for $N \geq 1$ at various orders of the DE.

DE up to order $O(\partial^4)$ for critical exponents η , ν and ω . The raw data for these exponents obtained at successive orders of the DE (for the same regulators mentioned in previous sections) are presented in Table XVII and XVIII in Appendix A. For completeness, results from previous DE analysis are also included in these tables. The same considerations as for $N = 1$ and $N = 2$ applies here, concerning the strong indication that successive orders of the DE give bounds on exponents η and ν but not for ω . As such, we implement the “improved” version of central values and error estimates for the first two exponents but not for ω .

A special mention must be made for the calculation of error bars for the exponent ω . We employ the most conservative estimates for this exponent and a particular analysis (already discussed in Sect. IV C) must be done in that case. Indeed, as shown in Fig. V C, when varying N the exponent ω turns out to be relatively stable at orders $O(\partial^2)$ and $O(\partial^4)$ but varies in a very important way at order LPA. More importantly, the curve of orders LPA and $O(\partial^2)$ crosses in a point between $N = 3$ and $N = 4$. Similarly, the curves for orders $O(\partial^2)$ and $O(\partial^4)$ cross in a point for $N \sim 2$. These exceptional points where two consecutive orders of the DE cross can make the uncertainty presented in Sect. IV too optimistic. To avoid this artificially small error bar, we employ a conservative estimate of error bars explained in Sect. IV C. The corresponding results are presented in Tables VI and VII where, as before, they are compared to other results in the literature both theoretical and experimental.

We obtain again very precise estimates for the three exponents that, in some cases, are the most precise exponents obtained in the literature for these universality classes from field-theoretical methods. The results are in some cases even more precise than MC simulations. Moreover, all our results are compatible (within error bars) with the best estimates in the literature (whenever more precise results than ours are available). This is a strong indication that our estimates of error bars are reli-

TABLE VI. Final results at various orders of the DE with appropriate error bars for $N = 3$ in $d = 3$. For reference results of CB ([53] for η and ν and [55] for ω), MC ([60] for η and ν and [61] for ω), combined MC and High-Temperature analysis from [62], and 6-loop, $d = 3$ perturbative RG values [2], and ϵ -expansion at order ϵ^5 [2] and order ϵ^6 [48] are also given for comparison. Results for most precise experiments are also included (Isotropic ferromagnets Gd_2BrC and Gd_2IC from [63] and CdCr_2Se_4 from [64]). Whenever needed, scaling relations are used in order to express results in terms of η and ν .

	ν	η	ω
LPA	0.7620	0	0.702
$O(\partial^2)$	0.7125(71)	0.0408(58)	0.754(34)
$O(\partial^4)$	0.7114(9)	0.0376(13)	0.769(11)
CB	0.7120(23)	0.0385(13)	0.791(22)
6-loop $d = 3$	0.7073(35)	0.0355(25)	0.782(13)
ϵ -expansion, ϵ^5	0.7045(55)	0.0375(45)	0.794(18)
ϵ -expansion, ϵ^6	0.7059(20)	0.0378(5)	0.795(7)
MC	0.7116(10)	0.0378(3)	0.773
MC+High-T.	0.7112(5)	0.0375(5)	
Ferromagnet Gd_2BrC	0.7073(43)	0.032(10)	
Ferromagnet Gd_2IC	0.7067(60)	0.061(15)	
Ferromagnet CdCr_2Se_4	0.656(56)	0.041(23)	

TABLE VII. Final results at various orders of the DE with appropriate error bars for $N = 4$ in $d = 3$. For reference results of CB (η and ν from [65] and ω from [55]), MC (η and ν from [66] and ω from [61]), and 6-loop, $d = 3$ perturbative RG values [2] and ϵ -expansion at order ϵ^5 [2] and order ϵ^6 [48] and are also given for comparison.

	ν	η	ω
LPA	0.805	0	0.737
$O(\partial^2)$	0.749(8)	0.0389(56)	0.731(34)
$O(\partial^4)$	0.7478(9)	0.0360(12)	0.761(12)
CB	0.7472(87)	0.0378(32)	0.817(30)
6-loop $d = 3$	0.741(6)	0.0350(45)	0.774(20)
ϵ -expansion, ϵ^5	0.737(8)	0.036(4)	0.795(30)
ϵ -expansion, ϵ^6	0.7397(35)	0.0366(4)	0.794(9)
MC	0.7477(8)	0.0360(4)	0.765

able. In Table VI experimental results are also presented for various physical realizations of $N = 3$ universality class. As for $N = 2$, the experimental precision for the exponent η is much lower than for exponent ν .

D. The large N case

Even if the $N = 5$ has been proposed to describe a possible universality class in some superconductors [3], the main purpose of the present section is to test our DE results in a limit where different kinds of approxi-

mations have been implemented, including the Large- N expansion. In fact, the expressions for the critical exponents η , ν and ω , in this limit have been computed at next-to-next-to-leading order [67–69] :

$$\begin{aligned}
 \eta &= \frac{8}{3\pi^2} \frac{1}{N} - \frac{512}{27\pi^4} \frac{1}{N^2} - \frac{8}{27\pi^6 N^3} \\
 &\quad \times \left[\frac{797}{18} - \zeta(2) \left(27 \log(2) - \frac{61}{4} \right) + \zeta(3) \frac{189}{4} \right] + \mathcal{O}(1/N^4) \\
 \nu &= 1 - \frac{32}{3\pi^2} \frac{1}{N} - \frac{128}{27\pi^4} \left(-112 + 27\pi^2 \right) \frac{1}{N^2} + \mathcal{O}(1/N^3) \\
 \omega &= 1 - \frac{64}{3\pi^2} \frac{1}{N} + \frac{128}{9\pi^4} \frac{1}{N^2} \left(\frac{104}{3} - \frac{9\pi^2}{2} \right) + \mathcal{O}(1/N^3)
 \end{aligned} \tag{29}$$

We used these expressions as reference values. As well known, the large- N expansion is expected to be a good approximation only for N larger than about ten. However, for reference, we compare also to this expansion in the $N = 5$ case. In order to estimate central values and error bars of the $1/N$ expansion, we use a very conservative estimate: we choose as central value the exponent obtained at the highest known order in the $1/N$ expansion and we estimate the error bar as the difference between this order and the previous one. This estimate may be too pessimistic for N large enough and the actual error bars at $N = 20$ or 100 could be smaller. However, given that coefficients in the large- N expansion are typically not of order one, we employed this conservative estimate. It is important to note that even with such conservative error bars some results of the large- N expansion becomes incompatible with other estimates for $N = 5$ and 10 . For some of the considered values of N there are also available resummed 6-loops and MC results that we include for comparison.

In order to estimate our central values and error bars we employed for all the considered values of $N > 5$ and for the exponents ν and ω the most conservative estimate presented in Sects. IV A and IV C. The reason is that we do not have clear indications that for those values of N the estimates coming from the DE constitute bounds on those critical exponents. Even more, in some cases for $N \geq 10$ we observe overlaps between the values obtained in consecutive orders of the DE for these exponents, indicating that, at least for those orders and values of $O(\partial^4)$, the hypothesis of being bounds is not fulfilled, see Fig. 5. The case of the exponent η is different because we observe the same qualitative behavior for all $N \geq 1$ which strongly indicates that, at least up to order $O(\partial^4)$, the estimates are bounds on the exponents (as a typical example, see Fig. 5). In any case, the dependence on regulator families and on the regulating function parameter α becomes much less pronounced for N large enough. Accordingly, the relevance of the precise choice of regulator becomes less important. Our results turn out to be mostly compatible with other estimates in the literature and seem to be even more precise. Indeed, only for very large values of N – of order 20 – the $1/N$ expansion becomes more precise than our $\mathcal{O}(\partial^4)$ results.

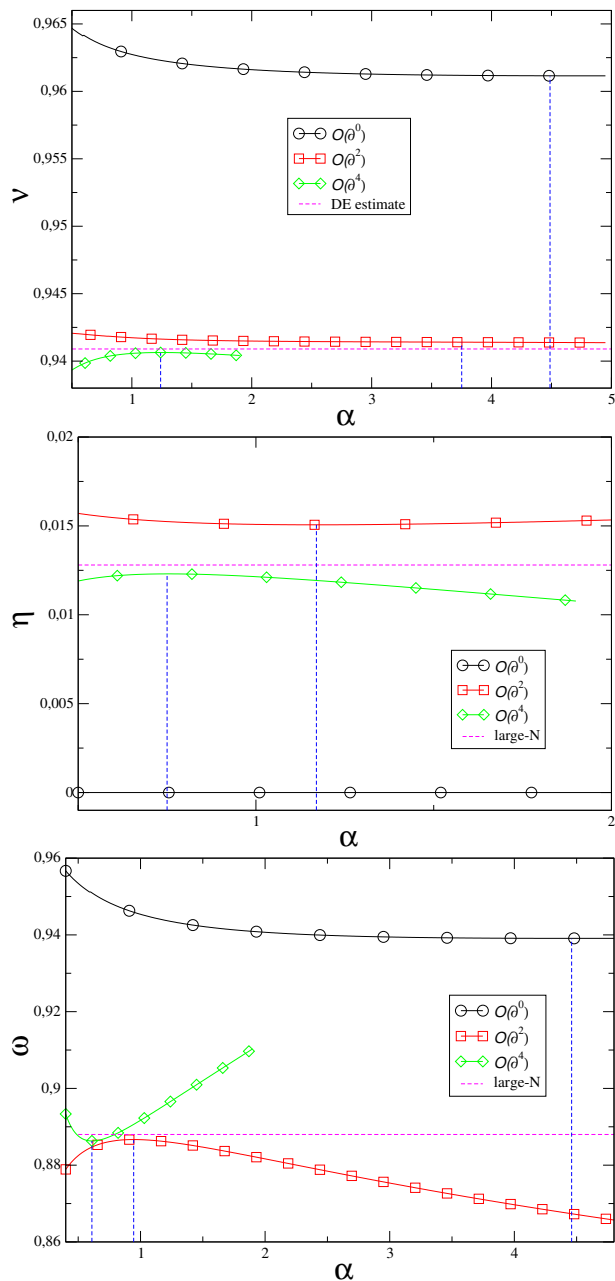


FIG. 5. From top to bottom: exponents ν , η and ω as a function of α for $N = 20$ for the regulating function (25c).

Of course, as is well known, the large N limit is obtained exactly [28] with the DE already at order LPA, but we also observe that $1/N$ corrections seem to be very well estimated at order $\mathcal{O}(\partial^4)$.

E. Analysis of some non-unitary cases: $N = 0$ and $N = -2$

In this section we consider two cases of $O(N)$ models for non-positive values of N . These are interesting for two different reasons. First, they describe situations of phys-

TABLE VIII. Final results at various orders of the DE with appropriate error bars for $N = 5$ in $d = 3$. For reference results of MC [70], Large- N expansion [67–69] and 6-loop, $d = 3$ perturbative RG values [71] are also given for comparison.

	ν	η	ω
LPA	0.839	0	0.770
$\mathcal{O}(\partial^2)$	0.782(8)	0.0364(52)	0.724(34)
$\mathcal{O}(\partial^4)$	0.7797(9)	0.0338(11)	0.760(18)
6-loop $d = 3$	0.766	0.034	
MC	0.728(18)		
Large- N	0.71(7)	0.031(15)	0.51(6)

TABLE IX. Final results at various orders of the DE with appropriate error bars for $N = 10$ in $d = 3$. For reference from Large- N expansion [67–69] and 6-loop, $d = 3$ perturbative RG values [71] are also given for comparison.

	ν	η	ω
LPA	0.919	0	0.874
$\mathcal{O}(\partial^2)$	0.877(11)	0.0240(34)	0.788(26)
$\mathcal{O}(\partial^4)$	0.8776(10)	0.0231(6)	0.807(7)
6-loop $d = 3$	0.859	0.024	
Large- N	0.87(2)	0.023(2)	0.77(1)

ical interest. $N = 0$ corresponds to self-avoiding walks [20] which model long polymer chain with self-repulsion. The case $N = -2$ corresponds to loop-erased random walks [72]. In such a random walk every loop is erased when it is formed. Second, these cases are interesting because unitarity is probably not valid when N is not a positive integer. Indeed, for positive integer values of N and d , $O(N)$ models have a clear interpretation in terms of a Ginzburg-Landau field theory verifying reflection-positivity. However, in the cases that are obtained by analytical continuation, the validity of unitarity of the Minkowskian version of the model is far from obvious. Since unitarity was explicitly used in the proof of the convergence of DE, we have to analyze the convergence

TABLE X. Final results at various orders of the DE with appropriate error bars for $N = 20$ in $d = 3$. For reference results of CB [65], Large- N expansion [67–69] and 6-loop, $d = 3$ perturbative RG values [71] are also given for comparison.

	ν	η	ω
LPA	0.9610	0	0.938
$\mathcal{O}(\partial^2)$	0.9414(49)	0.0130(19)	0.887(14)
$\mathcal{O}(\partial^4)$	0.9409(6)	0.0129(3)	0.887(2)
CB	0.9416(87)	0.0128(16)	
6-loop $d = 3$	0.930	0.014	
Large- N	0.941(5)	0.0128(2)	0.888(3)

TABLE XI. Final results at various orders of the DE with appropriate error bars for $N = 100$ in $d = 3$. For reference results from Large- N expansion [67–69] is also given for comparison.

	ν	η	ω
LPA	0.9925	0	0.9882
$O(\partial^2)$	0.9892(11)	0.00257(37)	0.9782(26)
$O(\partial^4)$	0.9888(2)	0.00268(4)	0.9770(8)
Large- N	0.9890(2)	0.002681(1)	0.9782(2)

properties in this situation. In this sense, the cases $N = 0$ and $N = -2$ can be seen as benchmarks for non-unitary theories. A similar issue occurs in the case of analytical continuation to non-integer d . It has been pointed out that unitarity is lost [73] in this situation, which makes the CB program more difficult to implement (at least with the same level of rigor as for positive integer values of d).

Let us mention, however, that the estimates on the convergence of the DE from Ref. [19] do not rely on all the information coming from the structure of a unitary theory but only on the position of singularities on the complex plane of squared momenta. In particular, at all orders of perturbation theory, these singularities are located, for all values of N including negative values, at the same positions as for unitary theories. As a consequence, at least at all orders of perturbation theory, one should expect that our estimate of the convergence of the DE and the existence of a small parameter should remain correct. Of course, the information coming from unitarity is that this structure remains correct non-perturbatively. Another information that comes from unitarity is that series for correlation functions are alternating (at least at large order). This comes from the fact that it is dominated by the 2 or 3-particles threshold which has a definite sign due to unitarity. For N that are not positive integers there is no reason at all to believe that successive orders of the DE give bounds on exponents. For example, see Fig. 6 where there is no indication of alternating values for ν (but the results for η does seem to alternate).

From a practical point of view we will continue to assume that there is a relative factor of order 4 that suppresses successive orders of the DE in order to estimate error bars but we will employ the more conservative estimate that do not assume that they give bounds on the exponents. The raw data obtained at various orders with various regulators are presented in Tables XV and XIV. They indicate that these assumptions seem to be justified. The results with corresponding error bars are presented in Tables XII and XIII which seem to confirm that our methodology for estimating errors (at least the most conservative version) remains valid for those non-positive values of N . It must be pointed out that the results of the CB for $N = 0$ are not as rigorous as for positive integer values of N . As a consequence, in this cases their

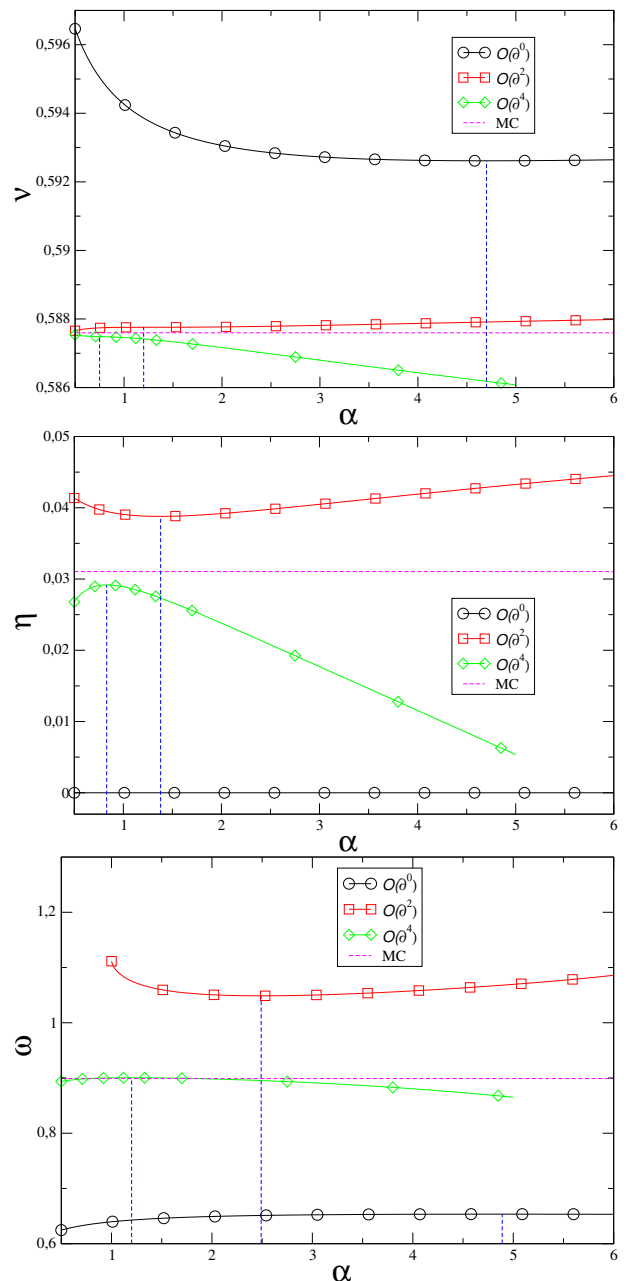


FIG. 6. From top to bottom: exponents ν , η and ω as a function of α for $N = 0$ for the regulating function (25c).

error bars does not constitute rigorous error bars. In Table XII we also compare to an experimental realization of the $N = 0$ case in a polymer solution [74].

A special mention must be done for some exact results known for the $N = -2$ case. In fact, the exponents η and ν are known exactly to take their mean-field value 0 and $1/2$. This result is well-known from an all-order perturbative analysis (see, for example, [4]) but a nice proof going beyond perturbation theory has been proposed recently [21, 22]. In these references, the exponent ω (which is not known exactly) is also estimated to be $\omega = 0.83 \pm 0.01$. It is interesting that the DE recovers

these results with high precision. Indeed, it was observed a long time ago that the LPA order reproduces the exact result for η and ν exactly for $N = -2$ [40]. However, the reason that makes the result exact at LPA order is somehow too simple. The fact, that $\eta = 0$ at LPA order is by construction true for any N . Therefore, its coincidence with the exact value for $N = -2$ is then an accident. Moreover, the flow of the mass term at zero field in LPA is controlled exclusively by the 4-point vertex at zero momenta and field which, for any N , verifies

$$\Gamma_{ijkl}^{(4)}(p_i = 0; \phi = 0) \propto (\delta_{ij}\delta_{kl} + \delta_{ik}\delta_{jl} + \delta_{il}\delta_{jk}). \quad (30)$$

Now, the flow of the mass at zero field is proportional to

$$\Gamma_{ijkk}^{(4)}(p_i = 0; \phi = 0) \propto \delta_{ij}(N + 2). \quad (31)$$

The consequence is that the mass parameter does not flow for $N = -2$ and then $\nu = 1/2$.

This simple analysis does not extend beyond LPA and the exactness of $\eta = 0$ and $\nu = 1/2$ is slightly spoiled by the DE approximation. In order to remain true, very non-trivial relations must be preserved along the flow that, given the analysis of [21, 22] must be exact but are only satisfied within DE (beyond LPA) approximately. The systematic errors seem to grow in the raw data when going from order $O(\partial^2)$ to order $O(\partial^4)$ as seen in Table XIV. Let us mention, however, that the relations $\eta = 0$ and $\nu = 1/2$ are extremely well satisfied and the exact values are obtained in all cases within the expected error bars as seen in Table XIII⁸. One must point out that the estimate of systematic error bars is, however, problematic for those exponents at $N = -2$. As mentioned in Sect. IV C, when two consecutive orders of the DE cross, our estimates of error bars are not justified and it is better to employ a “typical” value of error bars. In the present analysis we employ as “typical” value for these two exponents those of $N = 0$. For the non-trivial exponent ω one can employ without difficulty our error bar estimate and results are compatible, and with the same order of precision as, the one coming from perturbation theory.

The study of these two non-unitary models then suggests that the domain of application of our methodology for estimating error bars goes beyond the realm of unitary theories.

VI. CONCLUSION AND PERSPECTIVES

The DE of the NPRG equations has proved to be an approximation scheme which is versatile and capable of

TABLE XII. Final results at various orders of the DE with appropriate error bars for $N = 0$ in $d = 3$. For reference results of CB [75], MC [76, 77], Length doubling method series [78], and 6-loop, $d = 3$ perturbative RG values [2], and ϵ -expansion at order ϵ^5 [2] and order ϵ^6 [48] are also given for comparison. Results for most precise experiment are also included (polystyrene benzene dilute solutions [74]). Whenever needed, scaling relations are used in order to express results in terms of η and ν .

	ν	η	ω
LPA	0.5925	0	0.66
$O(\partial^2)$	0.5879(13)	0.0326(47)	1.00(19)
$O(\partial^4)$	0.5876(2)	0.0312(9)	0.901(24)
CB	0.5876(12)	0.0282(4)	
Series LDM	0.58785(40)	0.0327(22)	
MC	0.58759700(40)	0.0310434(30)	0.899(14)
6-loop $d = 3$	0.5882(11)	0.0284(25)	0.812(16)
ϵ -expansion, ϵ^5	0.5875(25)	0.0300(50)	0.828(23)
ϵ -expansion, ϵ^6	0.5874(3)	0.0310(7)	0.841(13)
Polymer solution	0.586(4)		

TABLE XIII. Final results at various orders of the DE with appropriate error bars for $N = -2$ in $d = 3$. For reference results from exact or perturbative results [21, 22].

	ν	η	ω
LPA	1/2	0	0.700
$O(\partial^2)$	0.5000(12)	0.0000(47)	0.84(19)
$O(\partial^4)$	0.5001(1)	0.0004(9)	0.838(24)
exact/ 6-loop	1/2	0	0.83(1)

tackling a very broad range of physical systems. However, until very recently, the success of such a method remained suspicious because of the apparent lack of a control parameter in order to estimate *a priori* the precision of the results. In a recent work [19] this important difficulty has been addressed and it was shown that the DE has a control parameter of order 1/9 to 1/4. This has been shown in two ways. First, on a theoretical basis, by considering the position of the singularities on the complex plane of 1PI correlation functions as a function of momenta. Second, by corroborating this general analysis with an empirical study of the precision of the DE at large order [$\mathcal{O}(\partial^6)$] when applied to the critical regime of a Ginzburg-Landau model in the Ising universality class.

In the present article we used this general analysis to study the critical exponents η , ν and ω of an important family of critical phenomena characterized by $O(N)$ -invariant Ginzburg-Landau models. Previous studies performed within the DE at order $\mathcal{O}(\partial^2)$ had shown good precision but in the present work we show that when going to order $\mathcal{O}(\partial^4)$ one achieves, in most cases, the best precision for those systems with field-theoretical meth-

⁸ It is interesting to observe that, apparently, the distance with exact results is as expected at order $O(\partial^4)$ but is abnormally small at order $O(\partial^2)$ (see Table XIV). We do not have an explanation for such high precision at order $O(\partial^2)$.

ods⁹. In some cases we were even able to attain a better precision than Monte-Carlo estimates. In order to perform this analysis we developed a systematic procedure to compute error bars within the DE. This procedure was corroborated by a careful analysis of the very precisely studied Ising universality class (corresponding to $N = 1$) obtained in Ref. [19] and extending it to various values of N in the three-dimensional case.

An important application is the analysis of the $O(2)$ or XY model where a longstanding controversy exists between experiments [23] and the state-of-the-art Monte-Carlo estimates [8, 51, 52] and very recent results from the CB [24] for the specific heat α (or, equivalently, the correlation length exponent, ν). Most theoretical estimates, based on fixed dimension re-summed perturbation theory, ϵ -expansion or previous CB works were unable to achieve a precision high enough to disentangle between the estimates of experiments and simulations. Our results are in agreement with Monte-Carlo simulations and new CB results but exclude the results obtained with Helium-4 in micro-gravity. This result can be interpreted in many ways. One possible explanation is the one proposed in [53]: It could be that the analysis of the experimental data made in Ref. [23] underestimate error bars. Alternatively we could consider other possible sources of systematic errors in the experiment whose exceptional realization in micro-gravity makes difficult to repeat. Another possible explanation, but much more challenging from the theoretical viewpoint could be that for some unexplained reason the $O(2)$ model does not describe properly the Helium-4 critical point. This is difficult to believe because scale-invariant theories are typically a discrete set and there is no doubt that the $O(2)$ model describes at least three digits of critical exponents of Helium-4 superfluid transition. This explanation would require another scale-invariant model extremely close to but different from the $O(2)$ model. In any case, the agreement between two independent theoretical estimates pushes in favour of a new realization of the experiment in order to confirm or discard previous experimental results.

The results of the present article paves the way towards many applications in the near future. First, the methodology used to estimate error bars within the DE can be applied in many applications within NPRG [even at order $\mathcal{O}(\partial^2)$]. Second, this analysis of error estimates, even if probably very pessimistically, applies also to other approximation schemes such as the Blaizot-Méndez-Wschebor scheme [29, 30, 43]. This possibility should be exploited because many finite momentum physical properties are beyond the reach of the DE. Third, in the present article we only considered the

two independent dominant exponents and the correction to scaling exponent of $O(N)$ universality class at order $\mathcal{O}(\partial^4)$. It is clear that with the same methodology we can analyze a very broad set of universal and non-universal properties of $O(N)$ models well studied in the literature with other methods (see, for example, [3] for many universal aspects that could be analyzed with the present setup). Given the precision reached for leading critical exponents is to be expected that we can improve for several quantities the best current theoretical estimates by using the DE at order $\mathcal{O}(\partial^4)$. Fourth, on more fundamental aspects, the present analysis is strongly based on the use of “Principle of Minimal Sensitivity” that turned out to improve significantly the results of the DE but requires a more solid theoretical basis. In this sense, an important under-exploited information that could bring some clarity on this point may come from the use of conformal symmetry that, up to now, has almost not been exploited in the NPRG context in order to improve physical predictions (see, however, [35, 47, 79–81]).

ACKNOWLEDGMENTS

This work was supported by Grant 412FQ293 of the CSIC (UdelaR) Commission and Programa de Desarrollo de las Ciencias Básicas (PEDECIBA), Uruguay and ECOS Sud U17E01. IB acknowledges the support of the Croatian Science Foundation Project IP-2016-6-7258 and the QuantiXLie Centre of Excellence, a project cofinanced by the Croatian Government and European Union through the European Regional Development Fund - the Competitiveness and Cohesion Operational Programme (Grant KK.01.1.1.01.0004). NW also thanks the LPTMC for its hospitality and the CNRS for funding during the autumn of 2019. The authors would like to thank B. Delamotte for a detailed reading of a previous version of this manuscript.

Appendix A: Raw data for DE estimates of critical exponents

In this Appendix we present the raw data for exponents ν , η and ω obtained for various values of N with the regulators presented in Eqs. (25) (in the case of Θ^n regulators we present in all cases the results for $n = 3$ since for this value of n the DE is well behaved until order $\mathcal{O}(\partial^4)$ and, for $N = 1$, it turned out to be optimum at that order). For almost all cases, the results are presented at a PMS, determined as an extremum of the corresponding exponent as a function of α for each regulator. The only exceptions are marked with an asterisk in the tables. In those cases, there are no PMS for some particular exponents. In order to choose a particular value of α when no standard PMS is present, we extend the philosophy of PMS which requires the “minimum sensitivity”. When no extremum is present, we verified in each case that the

⁹ The only exceptions are the $N = 1$ [11–13] and $N = 2$ cases [24] in which quasi-exact results of the CB are available and for very large values of N ($N \gtrsim 20$) where the large- N expansion becomes very precise [67–69].

TABLE XIV. Raw data for $N = -2$ critical exponents in $d = 3$ obtained with various regulators at various orders of the DE.

regulator		ν	η	ω
LPA	W	1/2	0	0.7000
	Θ^3	1/2	0	0.7021
	E	1/2	0	0.6983
	Power-law [40]	1/2	0	
$O(\partial^2)$	W	$0.5 + 2.8 \times 10^{-8}$	5.9×10^{-8}	0.8451
	Θ^3	$0.5 + 5.9 \times 10^{-7}$	1.2×10^{-6}	0.8447
	E	$0.5 + 7.4 \times 10^{-8}$	1.3×10^{-7}	0.8446
$O(\partial^4)$	W	$0.5 + 7.0 \times 10^{-5}$	8.5×10^{-5}	0.8368
	Θ^3	$0.5 + 5.9 \times 10^{-5}$	9.7×10^{-5}	0.8344
	E	$0.5 + 8.5 \times 10^{-5}$	9.2×10^{-4}	0.8411

TABLE XV. Raw data for $N = 0$ critical exponents in $d = 3$ obtained with various regulators at various orders of the DE. When a value of α different of PMS is employed, this is explicitly indicated.

regulator		ν	η	ω
LPA	W	0.5925	0	0.6549
	Θ^1 [42]	0.5921	0	0.6579
	Θ^3	0.5923	0	0.6567
	E	0.5926	0	0.6535
	Power-law [40]	0.596	0	0.62
$O(\partial^2)$	W	0.5878 *	0.0384	1.0407
	W ($\alpha = 1$) [34]	0.590	0.039	
	Θ^3	0.5879	0.0373	0.9431
	E	0.5878 *	0.0388	1.0489
$O(\partial^4)$	W	0.5875 *	0.0299	0.9006
	Θ^3	0.5876 *	0.0303	0.9007
	E	0.5875 *	0.0292	0.9005

point with lower sensitivity, in the studied exponents to the parameter α corresponds to an inflexion point and, accordingly, we choose that value. We also included in the various tables previous DE results when available.

Appendix B: Numerical method

We describe in this section the details of the numerical method used to determine the fixed points and critical exponents at order $\mathcal{O}(\partial^s)$ of the DE approximation within the NPRG with $s = 0$, $s = 2$ and $s = 4$. The general structure of the procedure can be split in three steps: 1) deriving the flow equations of each function in the *ansatz* for the effective action; 2) finding the fixed point which governs the critical behavior of the system and 3) obtaining the critical exponents from the fixed point solution.

TABLE XVI. Raw data for $N = 2$ critical exponents in $d = 3$ obtained with various regulators at various orders of the DE. When a value of α different of PMS is employed, this is explicitly indicated.

regulator		ν	η	ω
LPA	W	0.7099	0	0.6717
	Θ^1 [42]	0.7082	0	0.6712
	Θ^3	0.7090	0	0.6715
	E	0.7106	0	0.6716
	Power-law [40]	0.73	0	0.66
$O(\partial^2)$	W	0.6669	0.0474	0.7983
	W ($\alpha = 1$) [34]	0.666	0.049	
	Θ^3	0.6673	0.0469	0.7992
	E	0.6663	0.0480	0.7972
	Power-law [40]	0.65	0.044	0.38
$O(\partial^4)$	W	0.6725	0.0361	0.7906
	Θ^3	0.6722	0.0367	0.7893
	E	0.6732	0.0350	0.7934

TABLE XVII. Raw data for $N = 3$ critical exponents in $d = 3$ obtained with various regulators at various orders of the DE. When a value of α different of PMS is employed, this is explicitly indicated.

regulator		ν	η	ω
LPA	W	0.7631	0	0.7019
	Θ^1 [42]	0.7611	0	0.6998
	Θ^3	0.7620	0	0.7010
	E	0.7639	0	0.7026
	Power-law [40]	0.78	0	0.71
$O(\partial^2)$	W	0.7047	0.0471	0.7541
	W ($\alpha = 1$) [34]	0.704	0.049	
	Θ^3	0.7054	0.0466	0.7563
	E	0.7039	0.0476	0.7516
$O(\partial^4)$	W	0.745	0.035	0.33
	W	0.7126	0.0358	0.7681
	Θ^3	0.7122	0.0363	0.7659
E	0.7136	0.0347	0.7729	

1. Deriving flow equations and truncation

In order to determine the flow equations for each of the function in the *ansatz* of the effective action Eq. (17), we compute from this *ansatz* the general n -point vertex function $\Gamma_{k i_1, \dots, i_n}^{(n)}$ and evaluate it in a homogeneous field configuration. As a rule of thumb for the DE approximation at order $\mathcal{O}(\partial^s)$, one needs to compute all n -point vertex functions up to $n = 2 + s$. Indeed, this is easy to understand by noticing that to isolate the flow of all functions, which are characterized by different internal indices and momentum structures, one needs to compute

TABLE XVIII. Raw data for $N = 4$ critical exponents in $d = 3$ obtained with various regulators at various orders of the DE. When a value of α different of PMS is employed, this is explicitly indicated.

regulator		ν	η	ω
LPA	W	0.8063	0	0.7370
	W ($\alpha = 1$) [34]	0.739	0.047	
	Θ^1 [42]	0.8043	0	0.7338
	Θ^3	0.8052	0	0.7354
	E	0.8071	0	0.7383
	Power-law [40]	0.824	0	0.75
$O(\partial^2)$	W	0.7405	0.0450	0.7310
	Θ^3	0.7412	0.0445	0.7340
	E	0.7396	0.0455	0.7274
	Power-law [40]	0.816	0.022	0.42
$O(\partial^4)$	W	0.7490	0.0343	0.7588
	Θ^3	0.7487	0.0348	0.7561
	E	0.7500	0.0332	0.7649

TABLE XIX. Raw data for $N = 5$ critical exponents in $d = 3$ obtained with various regulators at various orders of the DE. When a value of α different of PMS is employed, this is explicitly indicated.

regulator		ν	η	ω
LPA	W	0.8395	0	0.7706
	Θ^1 [42]	0.8377	0	0.7667
	Θ^3	0.8385	0	0.7687
	E	0.8402	0	0.7721
$O(\partial^2)$	W	0.7731	0.0420	0.7241
	Θ^3	0.7737	0.0416	0.7275
	E	0.7722	0.0425	0.7199
$O(\partial^4)$	W	0.7808	0.0323	0.7584
	Θ^3	0.7806	0.0327	0.7558
	E	0.7815	0.0313	0.7648

the flow of all vertex functions up to $\Gamma_k^{(s)}$. However, computing the flow of any $\Gamma_k^{(n)}$ involves the vertex functions $\Gamma_k^{(n+1)}$ and $\Gamma_k^{(n+2)}$.

We highlight that, when plugging in the vertex functions in the r.h.s. of the flow equations for the different $\Gamma_k^{(n)}$, we truncate the product of vertex functions *before expanding propagators* at order s . This is different from what was usually done in previous uses of the DE, where all terms coming from the product were taken into account leading to bigger equations (which are more complicate to handle). Anyway, although this could be done in principle, the difference between the two schemes are of order $\mathcal{O}(p^{s+2})$ which makes the shorter and simpler flow equations the selected option.

Finally, matching in the l.h.s. and in the r.h.s. of the flow equations the indices and momentum structures.

TABLE XX. Raw data for $N = 10$ critical exponents in $d = 3$ obtained with various regulators at various orders of the DE. When a value of α different of PMS is employed, this is explicitly indicated.

regulator		ν	η	ω
LPA	W	0.9194	0	0.8745
	Θ^1 [42]	0.9186	0	0.8713
	Θ^3	0.9190	0	0.8729
	E	0.9198	0	0.8758
	Power-law [40]	0.94	0	0.89
	$O(\partial^2)$	W	0.8774	0.0276
$O(\partial^2)$	W ($\alpha = 1$) [34]	0.881	0.028	
	Θ^3	0.8775	0.0274	0.7903
	E	0.8772	0.0279	0.7853
	Power-law [40]	0.95	0.0054	0.82
$O(\partial^4)$	W	0.8777	0.0222	0.8063
	Θ^3	0.8780	0.0225	0.8062
	E	0.8771	0.0218	0.8081

TABLE XXI. Raw data for $N = 20$ critical exponents in $d = 3$ obtained with various regulators at various orders of the DE. When a value of α different of PMS is employed, this is explicitly indicated.

regulator		ν	η	ω
LPA	W	0.9610	0	0.9384
	Θ^3	0.9608	0	0.9376
	E	0.9612	0	0.9391
	Power-law [40]	0.96	0	0.95
$O(\partial^2)$	W	0.9414 *	0.0149	0.8875
	Θ^3	0.9414	0.0148	0.8880
	E	0.9414 *	0.0151	0.8867
	Power-law [40]	0.98	0.0021	0.93
$O(\partial^4)$	W	0.9409	0.0125	0.8875
	Θ^3	0.9411	0.0126	0.8884
	E	0.9406	0.0123	0.8863

Allows to compute separately each of the flow equations for the different functions in the *ansatz*.

2. Finding the fixed point

There are two ways to go for finding the fixed point of the flow equations. The first one, which is more traceable to an experimental procedure, is to start from a microscopic theory or initial condition for $\Gamma_{k=\Lambda}$ and integrate the flow equation. One can do this for different values of the initial conditions and, in particular, vary or fine-tune one parameter. By a dichotomy procedure (which can be easily implemented by observing the flow of a certain quantity, say the derivative with respect to ρ of the

TABLE XXII. Raw data for $N = 100$ critical exponents in $d = 3$ obtained with various regulators at various orders of the DE. When a value of α different of PMS is employed, this is explicitly indicated.

regulator		ν	η	ω
LPA	W	0.9925	0	0.9882
	Θ^3	0.9924	0	0.9880
	E	0.9925	0	0.9883
	Power-law [40]	0.994	0	0.991
$O(\partial^2)$	W	0.98906	0.00308	0.9781
	W ($\alpha = 1$) [34]	0.990	0.0030	
	Θ^3	0.98933	0.00294	0.9782 *
	E	0.98908	0.00310	0.9781
$O(\partial^4)$	W	0.98884	0.00263	0.9771
	Θ^3	0.98888	0.00264	0.9772
	E	0.98877	0.00260	0.9767
	Power-law [40]	0.998	0.00034	0.988

potential at zero field), one can find an initial condition which leads the RG flow as close to the fixed point as required. This is equivalent to varying the temperature and measuring the system in order to find the critical temperature T_c . The other method, which is numerically more efficient, faster and more precise, consists in finding the zeros of the beta functions. There exist efficient root-finding procedures which work fine if one initializes the procedure sufficiently close to the fixed point. We will call this procedure the *root-finding* algorithm.

Since having a good initial condition from scratch is not simple, we combined both approaches. The procedure implemented was then to start with some value of N (say $N = 2$) and dimension d (we set from start $d = 3$ and never changed it) and start with a dichotomy procedure. This only takes a few hours in a personal computer if one takes a smart *ansatz* for the microscopic theory. After few dichotomies, the algorithm reaches a vicinity of the fixed point and the root-finding algorithm can be used. Once the fixed point is found, we use this as an initial condition for the root-finding procedure for another value of N (say 2.1) (Since the equations are well behaved for non-integer values, one can take small variations of N and/or d and trace the fixed point to a new value of interest of N and d .) In our particular case, we varied N and obtained the fixed point solution for all values of N considered in the article at $d = 3$. Each new value of N is obtained in a few minutes for a given regulator in a personal computer.

We discretized the ρ variable into a grid of $N_\rho = 40$ points and evolved the flow equations using a fourth order Runge-Kutta with fixed step with free boundary condi-

tions for the ρ direction. Because of the procedure used, there was no need to optimize in the time step taken, this part was merely to find a good enough fixed point solution for the root-finding part, which was implemented with a Newton-Raphson algorithm.

The normalization condition is fixed as $\tilde{Z}(\tilde{\rho}_i)|_{i=N_\rho/4} = 1$, where $\tilde{Z}(\tilde{\rho})$ is the dimensionless version of $Z_k(\rho)$ and $\tilde{\rho}_i$ is the value of $\tilde{\rho}$ at site i . On top of this, the size of the box L_ρ is adjusted for every N value in order for the minimum of the potential to fall always in the site $i = N_\rho/4$. From this definition, the value of η_k was extracted at every step of the procedure.

In all cases, the momentum integrals were performed using an adaptative 21 point Gauss-Kronrod quadrature rule (qags) provided in the quadpack library and ρ derivatives were approximated using a five point centered discretization except at the borders of the grid where five points were still used but, of course, not centered for the first two and last two points in the ρ grid.

3. Obtaining critical exponents

With a very precise fixed point solution we turn to finding the critical exponents. As just mentioned, η_k is extracted from the normalization condition and is obtained simultaneously with the fixed point solution. Indeed, the factor Z_k is the field renormalization which is related to the running anomalous dimension by $\partial_t Z_k = -\eta_k Z_k$ and when approaching the fixed point η_k approaches the field anomalous dimension η .

For the critical exponents ν and ω we performed a linear stability analysis around the fixed point. We computed the \mathcal{M} stability matrix by evaluating at perturbed position of the fixed point and computed the eigenvectors of the $13N_\rho - 1$ linear system (N_ρ variables for each function $U, Z, Y, W_1, \dots, W_{10}$). The -1 corresponds to the normalization condition which removes the variable attribute of $\tilde{Z}(\tilde{\rho}_i)|_{i=N_\rho/4} = 1$. The smallest eigenvalue λ_1 is identified with ν as $\lambda_1 = -\nu^{-1}$, while the second smallest eigenvalue is simply $\lambda_2 = \omega$.

We also tested that the results that we obtain by diagonalizing the stability matrix coincide with those corresponding, for example, to the evolution with t of the derivative of the potential with respect to ρ at zero field near the fixed point given by

$$U'_k(\rho = 0) \sim U'_*(\rho = 0) + A \exp(-t/\nu) + B \exp(t\omega) + \dots \quad (\text{B1})$$

All our results have been checked against changing parameters in order to use optimal or near optimal set of parameters. The extent of the field domain considered was also varied, as well as the accuracy with which integrals were calculated.

[1] K. G. Wilson and J. B. Kogut, Phys. Rept. **12**, 75 (1974).

[2] R. Guida and J. Zinn-Justin, J. Phys. **A31**, 8103 (1998),

- arXiv:cond-mat/9803240 [cond-mat].
- [3] A. Pelissetto and E. Vicari, *Physics Reports* **368**, 549 (2002).
 - [4] J. Zinn-Justin, *Quantum field theory and critical phenomena*, Vol. 113 (2002) pp. 1–1054.
 - [5] O. Schnetz, *Phys. Rev.* **D97**, 085018 (2018), arXiv:1606.08598 [hep-th].
 - [6] D. P. Landau and K. Binder, *A guide to Monte Carlo simulations in statistical physics* (Cambridge university press, 2014).
 - [7] M. Hasenbusch, *Phys. Rev. B* **82**, 174433 (2010).
 - [8] M. Hasenbusch, (2019), arXiv:1910.05916 [cond-mat.stat-mech].
 - [9] A. A. Belavin, A. M. Polyakov, and A. B. Zamolodchikov, *Nucl. Phys.* **B241**, 333 (1984), [605(1984)].
 - [10] P. Di Francesco, P. Mathieu, and D. Senechal, *Conformal Field Theory*, Graduate Texts in Contemporary Physics (Springer-Verlag, New York, 1997).
 - [11] S. El-Showk, M. F. Paulos, D. Poland, S. Rychkov, D. Simmons-Duffin, and A. Vichi, *Phys. Rev.* **D86**, 025022 (2012), arXiv:1203.6064 [hep-th].
 - [12] S. El-Showk, M. F. Paulos, D. Poland, S. Rychkov, D. Simmons-Duffin, and A. Vichi, *J. Stat. Phys.* **157**, 869 (2014), arXiv:1403.4545 [hep-th].
 - [13] F. Kos, D. Poland, and D. Simmons-Duffin, *JHEP* **11**, 109 (2014), arXiv:1406.4858 [hep-th].
 - [14] C. Wetterich, *Phys. Lett.* **B301**, 90 (1993), arXiv:1710.05815 [hep-th].
 - [15] U. Ellwanger, *Z. Phys.* **C58**, 619 (1993).
 - [16] T. R. Morris, *Int. J. Mod. Phys.* **A9**, 2411 (1994), arXiv:hep-ph/9308265 [hep-ph].
 - [17] J. Berges, N. Tetradis, and C. Wetterich, *Phys. Rept.* **363**, 223 (2002), arXiv:hep-ph/0005122 [hep-ph].
 - [18] B. Delamotte, *Lect. Notes Phys.* **852**, 49 (2012), arXiv:cond-mat/0702365 [cond-mat.stat-mech].
 - [19] I. Balog, H. Chat, B. Delamotte, M. Marohnic, and N. Wschebor, *Phys. Rev. Lett.* **123**, 240604 (2019), arXiv:1907.01829 [cond-mat.stat-mech].
 - [20] P. G. de Gennes, *Phys. Lett.* **A38**, 339 (1972).
 - [21] K. J. Wiese and A. A. Fedorenko, *Nucl. Phys.* **B946**, 114696 (2019), arXiv:1802.08830 [cond-mat.stat-mech].
 - [22] K. J. Wiese and A. A. Fedorenko, *Phys. Rev. Lett.* **123**, 197601 (2019), arXiv:1908.11721 [cond-mat.dis-nn].
 - [23] J. A. Lipa, J. A. Nissen, D. A. Stricker, D. R. Swanson, and T. C. P. Chui, *Phys. Rev. B* **68**, 174518 (2003).
 - [24] S. M. Chester, W. Landry, J. Liu, D. Poland, D. Simmons-Duffin, N. Su, and A. Vichi, “Carving out open space and precise $o(2)$ model critical exponents,” (2019), arXiv:1912.03324 [hep-th].
 - [25] J. Polchinski, *Nucl. Phys.* **B231**, 269 (1984).
 - [26] L. Canet, B. Delamotte, D. Mouhanna, and J. Vidal, *Phys. Rev.* **B68**, 064421 (2003), arXiv:hep-th/0302227 [hep-th].
 - [27] L. Canet, B. Delamotte, D. Mouhanna, and J. Vidal, *Phys. Rev.* **D67**, 065004 (2003), arXiv:hep-th/0211055 [hep-th].
 - [28] M. D’Attanasio and T. R. Morris, *Phys. Lett.* **B409**, 363 (1997), arXiv:hep-th/9704094 [hep-th].
 - [29] J. P. Blaizot, R. Mendez Galain, and N. Wschebor, *Phys. Lett.* **B632**, 571 (2006), arXiv:hep-th/0503103 [hep-th].
 - [30] F. Benitez, J. P. Blaizot, H. Chate, B. Delamotte, R. Mendez-Galain, and N. Wschebor, *Phys. Rev.* **E85**, 026707 (2012), arXiv:1110.2665 [cond-mat.stat-mech].
 - [31] P. M. Stevenson, *Phys. Rev.* **D23**, 2916 (1981).
 - [32] C. Bervillier, *J. Phys. Condens. Matter* **17**, S1929 (2005), arXiv:hep-th/0501087 [hep-th].
 - [33] T. R. Morris and J. F. Tighe, *JHEP* **08**, 007 (1999), arXiv:hep-th/9906166 [hep-th].
 - [34] G. Von Gersdorff and C. Wetterich, *Phys. Rev.* **B64**, 054513 (2001), arXiv:hep-th/0008114 [hep-th].
 - [35] B. Delamotte, M. Tissier, and N. Wschebor, *Physical Review E* **93**, 012144 (2016).
 - [36] F. J. Wegner and A. Houghton, *Phys. Rev.* **A8**, 401 (1973).
 - [37] A. Hasenfratz and P. Hasenfratz, *Nucl. Phys. B* **270**, 687 (1986).
 - [38] N. Tetradis and C. Wetterich, *Nucl. Phys. B* **422**, 541 (1994).
 - [39] T. R. Morris, *Phys. Lett.* **B329**, 241 (1994), arXiv:hep-ph/9403340 [hep-ph].
 - [40] T. R. Morris and M. D. Turner, *Nucl. Phys.* **B509**, 637 (1998), arXiv:hep-th/9704202 [hep-th].
 - [41] S. Seide and C. Wetterich, *Nucl. Phys. B* **562**, 524 (1999).
 - [42] D. F. Litim, *Nucl. Phys. B* **631**, 128 (2002).
 - [43] F. Benitez, J.-P. Blaizot, H. Chaté, B. Delamotte, R. Mendez-Galain, and N. Wschebor, *Phys. Rev. E* **80**, 030103(R) (2009).
 - [44] T. R. Morris, *JHEP* **07**, 027 (2005), arXiv:hep-th/0503161 [hep-th].
 - [45] M. Tissier and G. Tarjus, *Physical Review B* **85** (2012), 10.1103/physrevb.85.104203.
 - [46] T. R. Morris, *Nucl. Phys.* **B458**, 477 (1996), arXiv:hep-th/9508017 [hep-th].
 - [47] G. De Polsi, M. Tissier, and N. Wschebor, *Journal of Statistical Physics* **177**, 1089 (2019).
 - [48] M. V. Kompaniets and E. Panzer, *Phys. Rev.* **D96**, 036016 (2017), arXiv:1705.06483 [hep-th].
 - [49] D. Simmons-Duffin, *JHEP* **03**, 086 (2017), arXiv:1612.08471 [hep-th].
 - [50] M. Campostrini, A. Pelissetto, P. Rossi, and E. Vicari, *Phys. Rev.* **E65**, 066127 (2002), arXiv:cond-mat/0201180 [cond-mat].
 - [51] M. Campostrini, M. Hasenbusch, A. Pelissetto, and E. Vicari, *Physical Review B* **74** (2006), 10.1103/physrevb.74.144506.
 - [52] W. Xu, Y. Sun, J.-P. Lv, and Y. Deng, *Phys. Rev.* **B100**, 064525 (2019), arXiv:1908.10990 [cond-mat.stat-mech].
 - [53] F. Kos, D. Poland, D. Simmons-Duffin, and A. Vichi, *JHEP* **08**, 036 (2016), arXiv:1603.04436 [hep-th].
 - [54] T.-Y. Lan, Y.-D. Hsieh, and Y.-J. Kao, “High-precision monte carlo study of the three-dimensional xy model on gpu,” (2012), arXiv:1211.0780 [cond-mat.stat-mech].
 - [55] A. C. Echeverri, B. von Harling, and M. Serone, *Journal of High Energy Physics* **2016**, 97 (2016).
 - [56] A. Singaas and G. Ahlers, *Phys. Rev. B* **30**, 5103 (1984).
 - [57] A. Oleaga, A. Salazar, and Y. M. Bunkov, *Journal of Physics: Condensed Matter* **26**, 096001 (2014).
 - [58] A. Oleaga, A. Salazar, D. Prabhakaran, J.-G. Cheng, and J.-S. Zhou, *Phys. Rev. B* **85**, 184425 (2012).
 - [59] R. Reisser, R. Kremer, and A. Simon, *Physica B: Condensed Matter* **204**, 265 (1995).
 - [60] M. Hasenbusch and E. Vicari, *Phys. Rev. B* **84**, 125136 (2011).
 - [61] M. Hasenbusch, *Journal of Physics A: Mathematical and General* **34**, 82218236 (2001).
 - [62] M. Campostrini, M. Hasenbusch, A. Pelissetto, P. Rossi, and E. Vicari, *Physical Review B* **65**

- (2002), 10.1103/physrevb.65.144520.
- [63] R. Reisser, R. K. Kremer, and A. Simon, *Phys. Rev. B* **52**, 3546 (1995).
 - [64] Zhang, Lei, Fan, Jiyu, Li, Li, Li, Renwen, Ling, Langsheng, Qu, Zhe, Tong, Wei, Tan, Shun, and Zhang, *EPL* **91**, 57001 (2010).
 - [65] F. Kos, D. Poland, D. Simmons-Duffin, and A. Vichi, *JHEP* **11**, 106 (2015), arXiv:1504.07997 [hep-th].
 - [66] Y. Deng, *Phys. Rev. E* **73**, 056116 (2006).
 - [67] Y. Okabe and M. Oku, *Progress of Theoretical Physics* **60**, 1287 (1978), <http://oup.prod.sis.lan/ptp/article-pdf/60/5/1287/5192266/60-5-1287.pdf>.
 - [68] A. N. Vasil'ev, Y. M. Pis'mak, and Y. R. Khonkonen, *Theoretical and Mathematical Physics* **50**, 127 (1982).
 - [69] D. J. Broadhurst, J. A. Gracey, and D. Kreimer, *Z. Phys.* **C75**, 559 (1997), arXiv:hep-th/9607174 [hep-th].
 - [70] X. Hu, *Physical Review Letters* **87** (2001), 10.1103/physrevlett.87.057004.
 - [71] S. A. Antonenko and A. I. Sokolov, *Physical Review E* **51**, 18941898 (1995).
 - [72] G. F. Lawler, *Duke Math. J.* **47**, 655 (1980).
 - [73] M. Hogervorst, S. Rychkov, and B. C. van Rees, *Phys. Rev.* **D93**, 125025 (2016), arXiv:1512.00013 [hep-th].
 - [74] Cotton, J.P., *J. Physique Lett.* **41**, 231 (1980).
 - [75] H. Shimada and S. Hikami, *J. Statist. Phys.* **165**, 1006 (2016), arXiv:1509.04039 [cond-mat.stat-mech].
 - [76] N. Clisby and B. Dünweg, *Phys. Rev. E* **94**, 052102 (2016).
 - [77] N. Clisby, *Journal of Physics A: Mathematical and Theoretical* **50**, 264003 (2017).
 - [78] R. D. Schram, G. T. Barkema, R. H. Bisseling, and N. Clisby, *Journal of Statistical Mechanics: Theory and Experiment* **2017**, 083208 (2017).
 - [79] O. J. Rosten, *Eur. Phys. J.* **C77**, 477 (2017), arXiv:1411.2603 [hep-th].
 - [80] O. J. Rosten, *Int. J. Mod. Phys.* **A34**, 1950027 (2019), arXiv:1605.01729 [hep-th].
 - [81] T. R. Morris and R. Percacci, *Phys. Rev.* **D99**, 105007 (2019), arXiv:1810.09824 [hep-th].